May 2003, LC-PHSM-2003-064
Phys. Lett. B 565 (2003) 42

Determining $\tan\beta$ with Neutral and Charged Higgs Bosons at a Future e^+e^- Linear Collider

J. Gunion[1], T. Han[2], J. Jiang[3], A. Sopczak[4]

[1]*Davis Institute for HEP, Univ. of California, Davis, CA 95616*
[2]*Dept. of Physics, Univ. of Wisconsin, Madison, WI 53706*
[3]*HEP Division, Argonne National Laboratory, Argonne, IL 60439*
[4]*Lancaster University, UK*

Abstract

The ratio of neutral Higgs field vacuum expectation values, $\tan\beta$, is one of the most important parameters to determine in either the Minimal Supersymmetric Standard Model (MSSM) or a general type-II Two-Higgs Doublet Model (2HDM). Assuming an energy and integrated luminosity of $\sqrt{s} = 500$ GeV and $\mathcal{L} = 2000$ fb^{-1} at a future linear collider (LC), we show that a very accurate determination of $\tan\beta$ will be possible for low and high $\tan\beta$ values by measuring the production rates of Higgs bosons and reconstructing Higgs boson decays. In particular, based on a TESLA simulation, and assuming no other light Higgs bosons and $100 \leq m_A \leq 200$ GeV, we find that the rate for the process $e^+e^- \to b\bar{b}A \to b\bar{b}b\bar{b}$ provides a good determination of $\tan\beta$ at high $\tan\beta$. In the MSSM Higgs sector, in the sample case of $m_A = 200$ GeV, we find that the rates for $e^+e^- \to b\bar{b}A + b\bar{b}H \to b\bar{b}b\bar{b}$ and for $e^+e^- \to HA \to b\bar{b}b\bar{b}$ provide a good determination of $\tan\beta$ at high and low $\tan\beta$, respectively. We also show that the direct measurement of the average total widths of the H and A in $e^+e^- \to HA \to b\bar{b}b\bar{b}$ events provides an excellent determination of $\tan\beta$ at large values. In addition, the charged Higgs boson process $e^+e^- \to H^+H^- \to t\bar{b}\bar{t}b$ has been studied. The sensitivity to $\tan\beta$ at the LHC obtained directly from heavy Higgs boson production is briefly compared to the LC results.

I INTRODUCTION

Theories beyond the Standard Model (SM) that resolve the hierarchy and fine-tuning problems typically involve extensions of its single-doublet Higgs sector to at least a two-doublet Higgs sector (2HDM) [1]. The most attractive such model is the Minimal Supersymmetric Standard Model (MSSM), which contains a constrained two-Higgs-doublet sector [2]. In other cases, the effective theory below some energy scale is equivalent to a 2HDM extension of the SM with no other new physics. Searching for the Higgs particles and studying their properties have high priority for both theoretical and experimental activities in high energy physics.

Among other new parameters in 2HDM and SUSY theories, one is of particular importance: the ratio of the vacuum expectation values of the two Higgs fields, commonly denoted as $\tan\beta = v_2/v_1$. It characterizes the relative fraction that the two Higgs doublets contribute to the electroweak symmetry breaking $v^2 = v_1^2 + v_2^2$, where $v \approx 246$ GeV. The five physical Higgs states couple to the fermions at tree-level [1, 2] as

$$h\bar{t}t : -i\frac{m_t}{v}\frac{\cos\alpha}{\sin\beta} \approx -i\frac{m_t}{v} \qquad h\bar{b}b : i\frac{m_b}{v}\frac{\sin\alpha}{\cos\beta} \approx -i\frac{m_b}{v} \tag{1}$$

$$H\bar{t}t : -i\frac{m_t}{v}\frac{\sin\alpha}{\sin\beta} \approx i\frac{m_t}{v}\cot\beta \qquad H\bar{b}b : -i\frac{m_b}{v}\frac{\cos\alpha}{\cos\beta} \approx -i\frac{m_b}{v}\tan\beta \tag{2}$$

$$A\bar{t}t : -\frac{m_t}{v}\cot\beta\,\gamma_5 \qquad A\bar{b}b : -\frac{m_b}{v}\tan\beta\,\gamma_5 \tag{3}$$

$$H^+\bar{t}b : i\frac{V_{td}}{\sqrt{2}v}[m_b\tan\beta(1+\gamma_5) + m_t\cot\beta(1-\gamma_5)], \tag{4}$$

where α is the mixing angle in the CP-even sector, and the approximation indicates the decoupling limit for $m_A \gg m_Z$ in the MSSM [3, 4], in which the couplings of the light Higgs boson h become SM-like. Eqs. (2)–(4) show that $\tan\beta$ governs the coupling strength of Yukawa interactions between the fermions and the heavy Higgs bosons. In fact, heavy Higgs boson measurements sensitive to their Yukawa couplings are far and away the most *direct* way to probe the structure of the vacuum state of the model as characterized by the ratio of vacuum expectation values that defines $\tan\beta$.

The parameter $\tan\beta$ enters all other sectors of the theory in a less direct way [1]. For instance, in supersymmetric theories the interactions of the SUSY particles have $\tan\beta$ dependence. In addition, the relations of SUSY particle masses to the soft SUSY breaking parameters of supersymmetry involve $\tan\beta$. The renormalization group evolution of the Yukawa couplings from the unification scale to the electroweak scale is sensitive to the value of $\tan\beta$. The large top quark mass can be naturally explained with $m_b - m_\tau$ unification as a quasi-infrared fixed point of the top Yukawa coupling if $\tan\beta \simeq 2$ or $\tan\beta \simeq 56$ [5]. The possibility of SO(10) Yukawa unification requires high $\tan\beta$ solutions [6]. The predicted mass of the lightest SUSY Higgs boson also depends on $\tan\beta$, with a higher mass at larger $\tan\beta$ [7]. It will be very important to compare the measurements of and constraints on $\tan\beta$ from these other sectors of the theory to the direct determination of $\tan\beta$ coming from the heavy Higgs boson measurements that depend fundamentally on $\tan\beta$ through the Yukawa couplings.

Currently, some regions of the MSSM parameter space have been excluded at LEP due to the lower bound on the lightest Higgs boson mass. (A review of LEP-1 Higgs results shows possible signatures for all neutral and charged Higgs boson search channels [8].) Particularly interesting is the exclusion $0.5 < \tan\beta < 2.4$ in the maximal-top-squark-mixing scenario when the SUSY scale $M_{\rm SUSY} \lesssim 1$ TeV [9]. More general MSSM parameter scans reduce the excluded $\tan\beta$ range [10], especially if the top quark mass is allowed to vary within its 1σ error range. Searches for top decay $t \to H^+ b$ at the Fermilab Tevatron, sensitive to $\tan\beta > 50$ with $m_t > m_{H^\pm}$, and searches for the final state $b\bar{b}h \to b\bar{b}b\bar{b}$, sensitive to $\tan\beta > 35$, have also set limits [11] on the very high values of $\tan\beta$ as a function of the Higgs mass. Precision electroweak measurements may provide some weak constraints on $\tan\beta$ [12]. Much of the parameter space, however, remains to be explored at future collider experiments.

Because of the significance of $\tan\beta$ for the theory and phenomenology, it is important to constrain it and eventually to determine its value in future collider experiments. At the upgraded Tevatron (Run II) with high luminosity (10 fb^{-1} or higher), complementarity among the processes $q\bar{q} \to Wh, Zh$ [13], $gg \to b\bar{b}h, b\bar{b}H, b\bar{b}A$ [14, 15], and $gg \to h, H, A \to \tau^+\tau^-$ [16] may allow SUSY Higgs detection throughout the full SUSY parameter $(m_A, \tan\beta)$ plane. Depending upon the integrated luminosity and the value of $\tan\beta$, either we will be able to directly observe the heavy Higgs processes and be able to determine $\tan\beta$ or, if the $H, A, H^\pm$ are not detected, we will be able to place an upper bound on $\tan\beta$ as a function of m_A. At high $\tan\beta$, SUSY particle production may provide an additional handle [17] for exploration of the parameters as well. More recently, it has been pointed out that a large value of $\tan\beta$ can substantially enhance B meson decay branching fractions [18] and thus could enhance our ability to probe SUSY parameters through indirect SUSY and Higgs signals [19]. SUSY Higgs detection at the LHC has been studied for many years; see [20] for a summary of the early work. Recent studies by the LHC CMS and ATLAS collaborations can be found in [21–23]. The conclusion of these studies is that there is a "no-lose" theorem for SUSY Higgs discovery at the LHC, although there is a substantial region of $(m_A, \tan\beta)$ parameter space where only the light CP-even h will be detected. The determination of $\tan\beta$ at the LHC by measuring Higgs boson production rates was analyzed in [20] and has been explored in greater detail in [22, 24]. The possibility of measuring $\tan\beta$ at the LHC via production of gauginos and squarks was explored in [25, 26]. A future linear collider has great potential for discovering new particles and measuring their properties due to its clean experimental environment. An early study [27] has been made to determine $\tan\beta$ via gaugino production in e^+e^- collisions, followed by a discussion for $e\gamma$ collisions [28]. In fact, the value of $\tan\beta$ can be analytically determined by measuring parameters in the gaugino sector of the MSSM, as outlined in [29]. Due to the clean experimental environment, stau pair production in e^+e^- collisions can be exploited to probe the SUSY parameters, in particular $\tan\beta$, via left-right mixing [30]. Especially useful at high $\tan\beta$ will be measurements of the τ polarization in $\tilde{\tau}$ decays, which is directly sensitive to $m_\tau/(\cos\beta m_W)$ [31].

Many SUSY particle production and decay processes depend on $\sin\beta$ or $\cos\beta$ (and not their inverses). Once $\tan\beta \gtrsim 5$, $\sin\beta \sim 1$ and $\cos\beta$ is simply small, and thus even large changes in $\tan\beta$ will have little impact on the related experimental observables at large $\tan\beta$ [28]. There are exceptions to this statement, including the τ polarization measurement referenced above. However, even this process involves other SUSY parameters at tree-level simultaneously as well. Thus, while many of the SUSY parameters can be measured with high precision, the accuracy with which $\tan\beta$ can be determined using measurements not involving the Higgs bosons remains uncertain, especially if $\tan\beta$ is large. Further, in non-SUSY extensions of the SM, it may be that the only direct probe of $\tan\beta$ will be via the Higgs sector. As seen from Eqs. (1)–(4), the heavy Higgs boson couplings to fermions are very sensitive to, and provide a direct probe of,

$\tan\beta$ at tree-level. Pair production of heavy Higgs bosons AH and H^+H^- was studied in e^+e^- collisions [32–34], and improved sensitivity to $\tan\beta$ was obtained by considering $H^\pm t\bar{b}$ [35] and $A/Hb\bar{b}, A/Ht\bar{t}$ [36]. If a muon collider becomes available to produce a heavy Higgs boson in the s-channel, its coupling could be measured with very excellent precision [37].

In this paper, we perform a comprehensive analysis of $\tan\beta$ determination via heavy Higgs boson production and decay at an e^+e^- linear collider with $\sqrt{s} = 500$ GeV and an integrated luminosity of 2000 fb^{-1}. We amplify upon the results for the heavy neutral Higgs bosons obtained during the last Snowmass workshop (as summarized in [38]) and extend our study to include the charged Higgs boson. We show how various Higgs boson measurements can be used to determine $\tan\beta$. The different types of measurements we consider are complementary in that some provide good precision at low $\tan\beta$ and others at high $\tan\beta$; combined, a good determination of $\tan\beta$ is possible throughout its whole range. We include background simulations and realistic b-tagging efficiencies. In Sec. II, we focus on the heavy Higgs bremsstrahlung process $b\bar{b}A \to b\bar{b}b\bar{b}$, the production rate for which is directly proportional to $\tan^2\beta$. We then include the $b\bar{b}H \to b\bar{b}b\bar{b}$ process in the context of the MSSM and estimate the accuracy with which $\tan\beta$ can be determined by combining experimental results for both processes. In Sec. III, we examine the pair production of a CP-even Higgs boson (h or H) and the CP-odd A, followed by decay of the Higgs bosons to the $b\bar{b}b\bar{b}$ final state. In particular, at large $\tan\beta$, the total decay widths of the heavy Higgs bosons can be broad since these widths are proportional to $\tan^2\beta$. The resulting accuracy for the $\tan\beta$ determination is obtained. We extend these studies to charged Higgs in Sec. IV. In Sec. V, we briefly summarize the LHC sensitivity to $\tan\beta$ deriving from heavy Higgs production. Finally, we summarize our results in Sec. VI.

Before proceeding with our analysis, we would like to point out that we are taking a phenomenological approach to the $\tan\beta$ determination. Namely, we only consider $\tan\beta$ as an effective way of specifying the coupling for the Higgs bosons and fermions through the usual tree-level relations and explore the extent to which this coupling can be experimentally determined at the linear collider experiments. After including radiative corrections, the relation of $\tan\beta$ to the various Yukawa couplings becomes process-dependent. For a recent theoretical discussion on the issue of the gauge dependence of these relations, see Ref. [39]. In this context, our results should be viewed as giving the accuracy with which the actual Yukawa couplings can be measured.

II THE $b\bar{b}A \to b\bar{b}b\bar{b}$ BREMSSTRAHLUNG PROCESS

Searches for $b\bar{b}A$ and $b\bar{b}h$ were performed in the four-jet channel using LEP data taken at the Z resonance [40–43]. In this section, we consider a linear collider with a center-of-mass energy of 500 GeV or higher, and begin by focusing just on the $b\bar{b}A$ production process that probes the direct coupling of the CP-odd Higgs A to $b\bar{b}$. Our analysis will employ cuts designed to eliminate Higgs pair resonant production, which, when kinematically accessible, dominates A production before cuts but is less sensitive to $\tan\beta$. The challenge of this study is the low expected production rate and the large irreducible background for a four-jet final state, as discussed in a previous study [44]. A LC analysis has been performed using event generators for the signal process $e^+e^- \to b\bar{b}A \to b\bar{b}b\bar{b}$ [45] and the $e^+e^- \to eW\nu,\ e^+e^-Z,\ WW,\ ZZ,\ q\bar{q}\ (q = u, d, s, c, b),\ t\bar{t},\ hA$ background processes [46] that include initial-state radiation and beamstrahlung.

For a 100 GeV CP-odd Higgs boson and $\tan\beta = 50$, the signal cross section is about 2 fb [47–49]. The generated events were passed through the fast detector simulation SGV [50]. The detector properties closely follow the TESLA detector Conceptual Design Report [51]. The

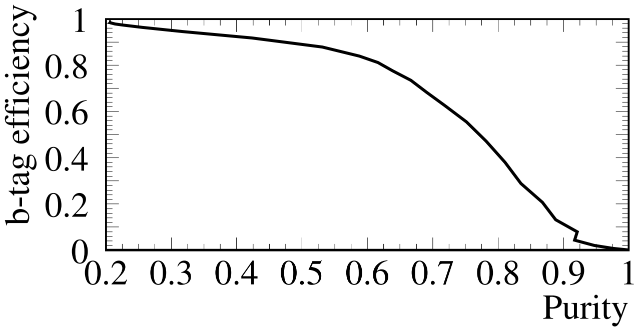

FIG. 1: Simulated b-tagging performance at the TESLA.

simulation of the b-tagging performance is very important for this analysis. The efficiency versus purity distribution for the simulated b-tagging performance is shown in Fig. 1 for the hadronic event sample $e^+e^- \to q\bar{q}$ for 5 flavors, where efficiency is the ratio of simulated $b\bar{b}$ events with the selection cuts to all simulated $b\bar{b}$ events, and purity is the ratio of simulated $b\bar{b}$ events with the selection cuts to all selected $q\bar{q}$ events. Details of the event selection and background reduction are described elsewhere [44].

For $m_A = 100$ GeV in the context of the MSSM, the SM-like Higgs boson is the H while the light h is decoupled from WW, ZZ [$\cos(\beta-\alpha) \sim 1$ and $\sin(\beta-\alpha) \sim 0$]. The $b\bar{b}h$ coupling is essentially equal (in magnitude) to the $b\bar{b}A$ coupling ($\propto \tan\beta$ at the tree level) and $m_h \sim m_A$, implying that the signal would be doubled from $b\bar{b}A$ and $b\bar{b}h$. Also important will be hA pair production, which is proportional to $\cos(\beta-\alpha)$ and will have full strength in this particular situation; HA production will be strongly suppressed. We focus first on $b\bar{b}A \to b\bar{b}b\bar{b}$.

The expected background rate for a given $b\bar{b}A \to b\bar{b}b\bar{b}$ signal efficiency is shown in Fig. 2. One component of the background is $hA \to b\bar{b}b\bar{b}$ since it has rather weak dependence on $\tan\beta$. Our selection procedures are, in part, designed to reduce this piece of the background as much as possible. Nonetheless, it may lead to significant systematic error in the determination of $\tan\beta$ due to interference with the signal, as discussed below. For the $b\bar{b}A \to b\bar{b}b\bar{b}$ signal, the sensitivity $S/\sqrt{B}$ for $m_A = 100$ GeV is almost independent of the working point choice of signal efficiency in the range $\epsilon_{\rm sel} = 5\%$ to 50%. For a working point choice of 10% efficiency, the total simulated background of about 16 million events is reduced to 100 background events with an equal number of signal events at $\tan\beta = 50$. We estimate the error on determining $\tan\beta$ by

$$\Delta\tan^2\beta/\tan^2\beta = \Delta S/S = \sqrt{S+B}/S. \tag{5}$$

If this were the only contributing process, then we would have $\sqrt{S+B}/S \approx 0.14$, resulting in an error on $\tan\beta = 50$ of 7%. For smaller values of $\tan\beta$, the sensitivity decreases rapidly. A 5σ signal detection is still possible for $\tan\beta = 35$. In the MSSM context, the $b\bar{b}h$ signal would essentially double the number of signal events and have exactly the same $\tan\beta$ dependence, yielding $\Delta\tan^2\beta/\tan^2\beta \sim \sqrt{300}/200 \sim 0.085$ for $\tan\beta = 50$.

Although the number of hA background events is very small compared to the other background reactions after the event selection, interference between the signal ($b\bar{b}A \to b\bar{b}b\bar{b}$ plus $b\bar{b}h \to b\bar{b}b\bar{b}$) and the background ($hA \to b\bar{b}b\bar{b}$) could be important. At the working point of 10% signal efficiency, and after applying the selection procedures, the expected rate for the latter is 2 ± 1 events for $\mathcal{L} = 500$ fb^{-1}. To assess the effect of the interference, let us momentarily retain only the $b\bar{b}A$ signal and the hA background. We first calculate the cross sections $\sigma(e^+e^- \to b\bar{b}A \to b\bar{b}b\bar{b})$, $\sigma(e^+e^- \to hA \to b\bar{b}b\bar{b})$, and $\sigma(e^+e^- \to b\bar{b}A + hA \to b\bar{b}b\bar{b})$ with

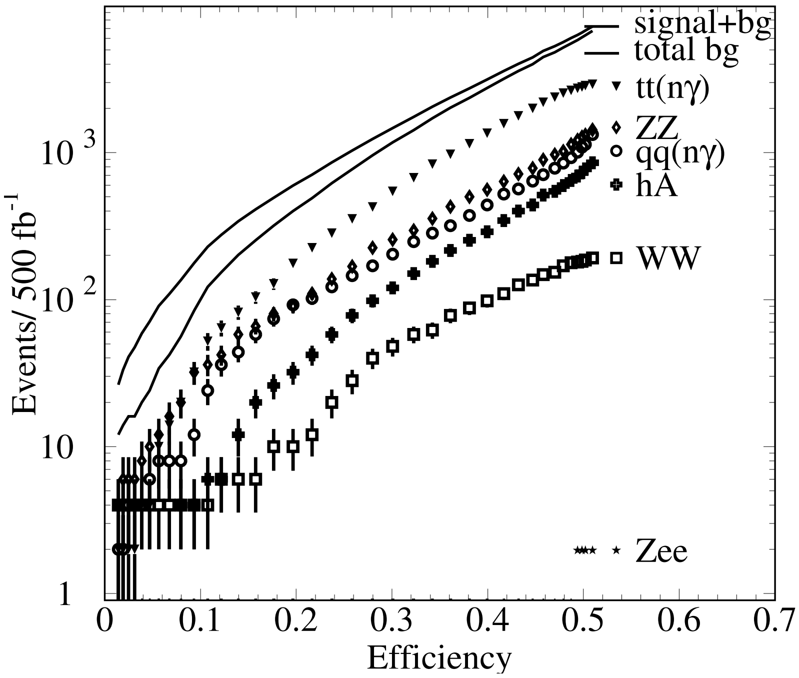

FIG. 2: Final background rate versus $b\bar{b}A$ signal efficiency for $m_A = 100$ GeV, $\sqrt{s} = 500$ GeV and $\mathcal{L} = 500$ fb^{-1}. We take a fixed value of $m_b = 4.62$ GeV.

CompHEP [52] before selections. We define the interference as

$$\sigma_{\rm interf} = \sigma_{b\bar{b}A+hA} - \sigma_{b\bar{b}A} - \sigma_{hA}. \tag{6}$$

For the default value $m_b = 4.62$ GeV, at $\tan\beta = 50$ we obtain $\sigma_{b\bar{b}A} = 1.83 \pm 0.01$ fb, $\sigma_{hA} = 36.85 \pm 0.10$ fb, $\sigma_{b\bar{b}A+hA} = 39.23 \pm 0.12$ fb, and thus $\sigma_{\rm interf} = 0.55 \pm 0.16$ fb. We observe a constructive interference similar in size to the signal. Thus, more signal events are expected than simulated and the statistical error estimate is conservative. After selection cuts, we have found 100 signal events versus two hA background events. The maximum interference magnitude arises if the interference events are signal-like, yielding an interference excess of $(10 + \sqrt{2})^2 - 100 - 2 \sim 28$, a percentage ($\sim 30\%$) similar to the ratio obtained before selection cuts. If the events from the interference are background-like, the resulting systematic error will be small, since the hA background is only a small part of the total background. In the MSSM context we have an exact prediction as a function of $\tan\beta$ for the combined contribution of $hA \to b\bar{b}b\bar{b}$ and $b\bar{b}A \to b\bar{b}b\bar{b}$ (plus $b\bar{b}h \to b\bar{b}b\bar{b}$), including all interferences, and this exact prediction can be compared to the data. In order to test this exact prediction, it may be helpful to compare theory and experiment for several different event selection procedures, including ones that give more emphasis to the hA process. Of course, this exact prediction depends somewhat on other MSSM parameters, especially if decays of the h or H to pairs of supersymmetric particles are allowed or ratios of certain MSSM parameters are relatively large [53]. If this type of uncertainty exists, the systematic error on $\tan\beta$ can still be controlled by simultaneously simulating all sources of $b\bar{b}b\bar{b}$ events for various $\tan\beta$ values and fitting the complete data set (assuming that the other MSSM parameters are known sufficiently well). Another possible theoretical systematic uncertainty derives from higher-order corrections. The full next-to-leading order (NLO) QCD corrections are given in [54, 55]. There it is found that using the running b-quark mass incorporates the bulk of the NLO corrections. For example, for $m_A = 100$ GeV, employing $m_b(100\text{ GeV}) \sim 2.92$ GeV versus $m_b(m_b) \sim 4.62$ GeV yields (before cuts) a cross section of

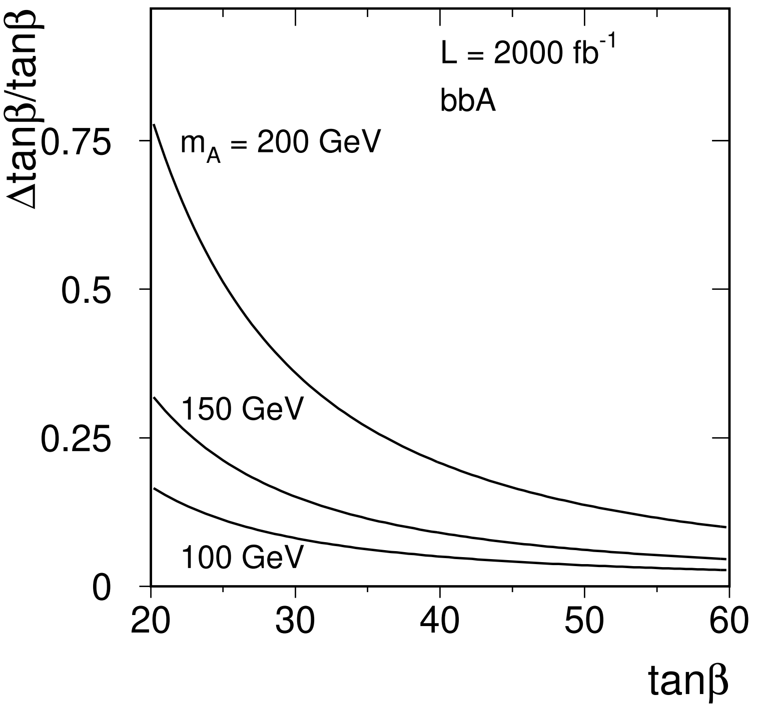

FIG. 3: The $\tan\beta$ statistical error for $\mathcal{L} = 2000$ fb^{-1} and $m_A = 100, 150, 200$ GeV for 10% selection efficiency. For $m_A = 100$ GeV, the signal and background rates are four times those given in Fig. 2 at the 10% efficiency point. Similar results are employed at $m_A = 150$ and 200 GeV.

~ 0.75 fb versus ~ 2 fb, respectively, at $\tan\beta = 50$. The signal rates and resulting errors quoted in this section are those computed using $m_b = 4.62$ GeV. Use of the running mass would reduce the event rates and increase our error estimates. In subsequent sections and figures, all results and errors are computed in the MSSM context using the running b-quark mass. Higher-order corrections of all kinds will be better known by the time the Linear Collider (LC) is constructed and data is taken and thus should not be a significant source of systematic uncertainty. An experimental challenge is associated with knowing the exact efficiency of the event selection procedure. At the working point of an efficiency $\epsilon_{\rm sel} = 10\%$, to achieve $\Delta\tan\beta/\tan\beta < 0.05$ requires $\Delta\epsilon_{\rm sel}/\epsilon_{\rm sel} < 0.1$, equivalent to $\Delta\epsilon_{\rm sel} < 1\%$.

In addition to the hA Higgs boson background, two other Higgs boson processes could lead to a $b\overline{b}b\overline{b}$ topology. First, the process $e^+e^- \to HZ$ can give a $b\overline{b}b\overline{b}$ final state. In fact, for large $\tan\beta$ the HZ cross section is maximal and similar in size to the hA cross section. Nonetheless, its contribution to the background is much smaller because the $HZ \to b\overline{b}b\overline{b}$ branching is below 10% compared to about 80% for $hA \to b\overline{b}b\overline{b}$. Since the hA process contributed only 2% of the total background, the contribution to the background from the HZ process can be neglected. The second Higgs boson process leading to a $b\overline{b}b\overline{b}$ topology is that already discussed, $e^+e^- \to b\overline{b}h$. The only distinction between this and the $e^+e^- \to b\overline{b}A$ process is a small difference in the angular distribution due to the different production matrix elements. Thus, the selection efficiency is almost identical. The production rate of the $b\overline{b}A$ process is proportional to $\tan^2\beta$ while the $b\overline{b}h$ production rate is proportional to $\sin^2\alpha/\cos^2\beta$. In the MSSM context, this latter factor is $\sim \tan^2\beta$ for $m_A \geq 100$ GeV and large $\tan\beta$ (assuming $M_{\rm SUSY} \sim 1$ TeV). In the general 2HDM, since $\tan\beta \approx 1/\cos\beta$ at large $\tan\beta$, the expected rate depends mostly on $\sin\alpha$ and the h mass. In this more general case where $m_h \approx m_A$ but the MSSM expectation of $\alpha \sim -\beta \sim -\pi/2$ does not hold, the enhancement of the $b\bar{b}A$ signal by the $b\bar{b}h$ addition would only allow a determination of $|\sin\alpha|$ as a function of the presumed value of $\tan\beta$ (using the constraint that one must obtain the observed number of $b\bar{b}h + b\bar{b}A$ events). Independent measurements of the HZ and hA production rates would then be needed to determine the value of $\beta - \alpha$ and only then could α and β be measured separately.

It is essential for the $\tan\beta$ determination that a very high integrated luminosity can be accumulated (we assume $\mathcal{L} = 2000$ fb^{-1} after several years of data-taking). Fig. 3 shows the expected statistical error on $\tan\beta$ for $m_A = 100, 150$ and 200 GeV, assuming that the only measured process is $b\bar{b}A$ with the help of our selection cuts. At the two higher m_A values, in the MSSM context it is the H that would be decoupled and have mass $m_H \sim m_A$ and the h would be SM-like. Consequently, the $b\bar{b}H$ rate would be essentially identical to the $b\bar{b}A$ rate and, assuming that one could verify the MSSM Higgs context by independent means, would lead to still smaller $\tan\beta$ statistical errors than plotted, the exact decrease depending upon the signal-to-background ratio. For $m_A = 150$ and 200 GeV, the HA process (like the hA process at $m_A = 100$ GeV) would have to be computed in a specific model context or its relative weight fitted by studying $b\bar{b}b\bar{b}$ production in greater detail in order to minimize any systematic error from this source. Results obtained in the case of the MSSM will be given in the following section.

III *HA* PRODUCTION: DECAY BRANCHING RATIOS AND TOTAL WIDTHS

The branching ratios for H, A and $H^\pm$ decay to various allowed modes vary rapidly with $\tan\beta$ in the MSSM when $\tan\beta$ is in the low to moderate range, roughly below 20. Consequently, if these branching ratios can be measured accurately, $\tan\beta$ can be determined with good precision in this range. Measurement of the branching fractions is most easily accomplished using HA and H^+H^- pair production. In particular, the pair production processes are nearly independent of $\tan\beta$ so that the rate in a given channel provides a fairly direct probe of the branching ratio for that channel. That $\tan\beta$ could be accurately determined using Higgs branching ratios measured in pair production was first demonstrated in [33, 34]. Refs. [33, 34] consider a number of models for which SUSY decays of the H, A and $H^\pm$ are kinematically allowed. It was found that by measuring all available ratios of branching ratios it was possible to determine $\tan\beta$ to better (often much better) than 10% for $\tan\beta$ values ranging from 2 up to as high as 25 to 30 for m_A in the 200–400 GeV range, assuming $\sqrt{s} = 1$ TeV and an effective luminosity (defined as the total luminosity times the selection efficiency of the cuts required to isolate the pair production process) of $\mathcal{L}_{\rm eff} = 80$ fb^{-1} (equivalent, for example, to $\mathcal{L} = 2000$ fb^{-1} for a selection efficiency of 4%). A more recent analysis using a few specific points in MSSM parameter space, focusing on the $b\bar{b}b\bar{b}$ event rate and including a study at $\sqrt{s} = 500$ GeV, is given in [36]. This latter study uses a selection efficiency of 13% and negligible background for detection of $e^+e^- \to hA \to b\bar{b}b\bar{b}$ (relevant for $m_A \leq 100$ GeV) or $e^+e^- \to HA \to b\bar{b}b\bar{b}$ (relevant for $m_A \geq 150$ GeV) and finds small errors for $\tan\beta$ at lower $\tan\beta$ values. Both [33, 34] and [36] assume MSSM scenarios in which there are significant decays of the A and H to pairs of SUSY particles, in particular neutralinos and charginos. These decays remain non-negligible up to fairly high $\tan\beta$ values. As a result, the $b\bar{b}$ branching fractions of the A and H increase more markedly as $\tan\beta$ increases than if SUSY decays are absent. Indeed, in the absence of SUSY decays, the $b\bar{b}b\bar{b}$ rate asymptotes quickly to a fixed value as $\tan\beta$ increases. As we shall see, this means that much smaller errors for the $\tan\beta$ determination using the $HA \to b\bar{b}b\bar{b}$ rate are achieved if SUSY decays are present.

We now examine the errors on $\tan\beta$ that could be achieved using Higgs pair production, following procedures related to those of [33, 34, 36], but using updated luminosity expectations and somewhat more realistic experimental assumptions and analysis techniques. We restrict the analysis to the process $e^+e^- \to HA \to b\bar{b}b\bar{b}$, ignoring possible additional sensitivity through ratios relative to other final states. With both Higgs bosons reconstructed in their $b\bar{b}$ final state as two back-to-back clusters of similar mass, backgrounds are expected to be negligible. All the results of this section are obtained using version 2.0 of HDECAY [56] for computing the branching ratios and total widths of the Higgs bosons.

To understand the sensitivity to the presence of SUSY decays of the heavy Higgs bosons, two different MSSM scenarios are considered:

(I) $m_A = 200$ GeV, $m_{\tilde{g}} = 1$ TeV, $\mu = M_2 = 250$ GeV,
$m_{\tilde{t}_L} = m_{\tilde{b}_L} = m_{\tilde{t}_R} = m_{\tilde{b}_R} \equiv m_{\tilde{t}} = 1$ TeV,
$A_\tau = A_b = 0$, $A_t = \mu/\tan\beta + \sqrt{6}m_{\tilde{t}}$ (maximal mixing);

(II) $m_A = 200$ GeV, $m_{\tilde{g}} = 350$ GeV, $\mu = 272$ GeV, $M_2 = 120$ GeV,
$m_{\tilde{t}_L} = m_{\tilde{b}_L} = 356$ GeV, $m_{\tilde{t}_R} = 273$ GeV, $m_{\tilde{b}_R} = 400$ GeV,
$A_\tau = 0$, $A_b = -672$ GeV, $A_t = -369$ GeV.

In scenario (I), SUSY decays of the H and A are kinematically forbidden. Scenario (II) is taken from [36] in which SUSY decays (mainly to $\widetilde{\chi}^0_1\widetilde{\chi}^0_1$) are allowed. We will assume that appropriate event selection criteria can be found such that for an event selection efficiency of 10% there will be negligible background. The resulting $HA \to b\bar{b}b\bar{b}$ event rates (per 2000 fb^{-1} of integrated luminosity) are plotted for $\sqrt{s} = 500$ GeV in Fig. 4 as a function of $\tan\beta$. The difference in the dependence of the event rates on $\tan\beta$ is apparent. In more detail: in scenario (I) the $b\bar{b}b\bar{b}$ event rates, after 10% selection efficiency, are 8, 77, 464, 1762, and 1859 at $\tan\beta = 1$, 2, 3, 10, and 40, respectively. The corresponding event rates in scenario (II) are 1, 5, 34, 1415 and 1842. These differing $\tan\beta$ dependencies imply significant sensitivity of the $\tan\beta$ errors to the scenario choice, with worse errors for scenario (I). Finally, we note that for $\tan\beta > 2$ the above event numbers are such that backgrounds are indeed negligible after 10% efficient selection cuts; for $\tan\beta \sim 1$, backgrounds might become an issue.

To determine the 1σ statistical errors of the $\tan\beta$ determination, we compute, for each choice of $\tan\beta$, the 1σ upper and lower bounds on the expected event number as $N(b\bar{b}b\bar{b}) \pm \sqrt{N(b\bar{b}b\bar{b})}$. These upper and lower bounds are also shown in Fig. 4. The upper (lower) event rate numbers are required to be ≥ 10 to set an upper (lower) $\tan\beta$ bound, respectively. Since the event number increases monotonically with $\tan\beta$ for both MSSM scenarios, we can then use the given MSSM model scenario to determine the $\tan\beta$ value for which the number of events is equal to the 1σ upper (lower) bound. These values define the 1σ upper (lower) bound on $\tan\beta$, respectively. The resulting fractional upper and lower limit errors $\Delta\tan\beta/\tan\beta$ are plotted for MSSM scenarios (I) and (II) in Fig. 5. This procedure assumes that other measurements of SUSY particle production at the LHC and the LC will have fixed the MSSM scenario.

Let us discuss in more detail the $\tan\beta$ errors from the $HA \to b\bar{b}b\bar{b}$ rate in scenario (II) as compared to scenario (I). From Fig. 4 we see that in scenario (I) once $\tan\beta$ reaches 10 to 12 the $b\bar{b}b\bar{b}$ rate will not change much if $\tan\beta$ is increased further since the $H \to b\bar{b}$ and $A \to b\bar{b}$ branching ratios approach constant values. In contrast, if $\tan\beta$ is decreased the $b\bar{b}b\bar{b}$ rate declines significantly as other decay channels come into play. Thus, meaningful lower bounds on $\tan\beta$ are retained out to relatively substantial $\tan\beta$ values whereas upper bounds on $\tan\beta$ disappear for $\tan\beta \gtrsim 10-12$. In scenario (II), for reasons explained below, we have not plotted

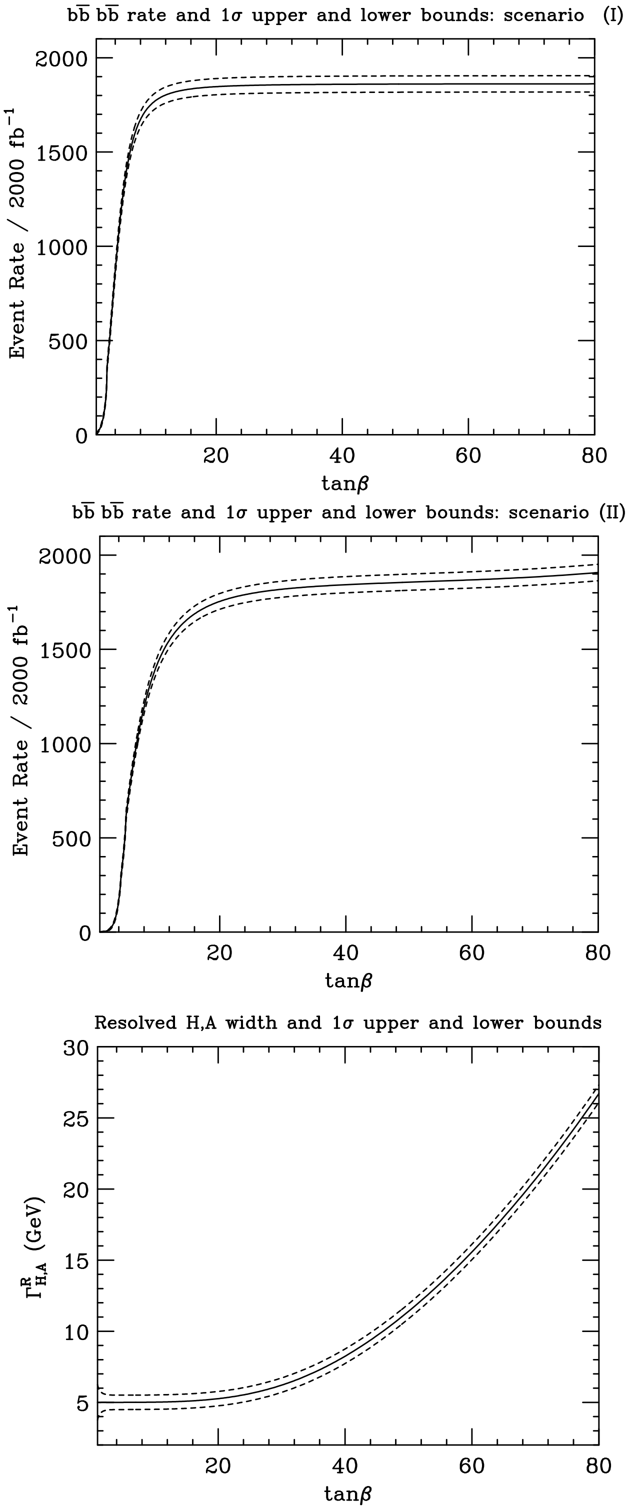

FIG. 4: Solid curves in the upper two figures give the rates for $e^+e^- \to HA \to b\bar{b}b\bar{b}$ in scenarios (I) and (II). The solid curve in the lower figure is the resolved width $\Gamma^{\rm R}_{H,A}$, Eq. (7), for scenario (I). Dashed curves in all three figures correspond to the 1σ upper and lower bounds on these quantities. We take $m_A = 200$ GeV, $\sqrt{s} = 500$ GeV and $\mathcal{L} = 2000$ fb^{-1}. An efficiency of 10% is assumed for cuts, acceptance and tagging. The upper and lower 1σ bounds for $\Gamma^{\rm R}_{H^\pm}$ include an additional efficiency factor of 0.75 for keeping only events in the central mass peak and assume the estimated mass resolution of $\Gamma_{\rm res} = 5$ GeV, including 10% systematic uncertainty. Results for $\Gamma^{\rm R}_{H,A}$ in SUSY scenario case (II) are very similar to those plotted for case (I). HDECAY [56] is used to compute the H and A widths and branching ratios.

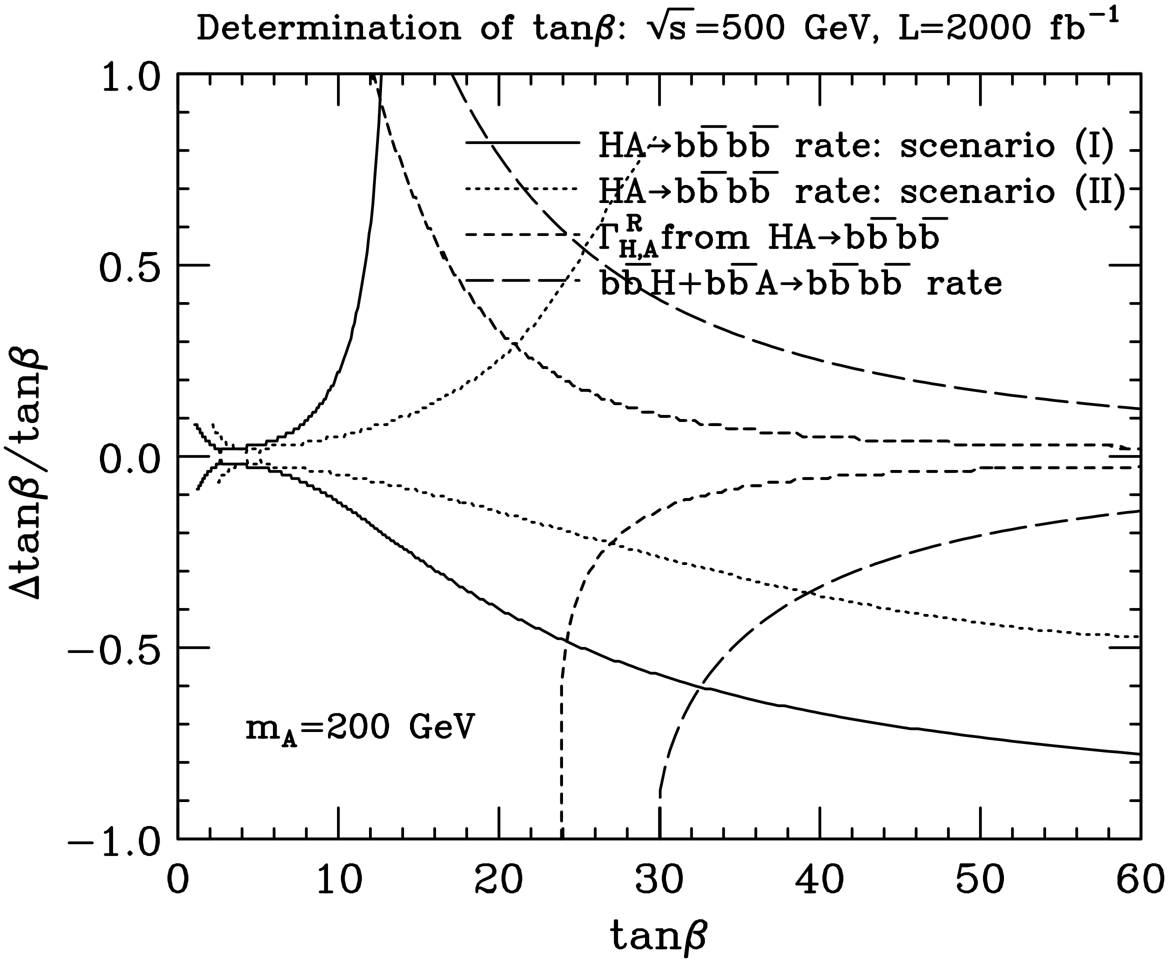

FIG. 5: For the MSSM with $m_A = 200$ GeV, and assuming $\mathcal{L} = 2000$ fb^{-1} at $\sqrt{s} = 500$ GeV, we plot the 1σ statistical upper and lower bounds, $\Delta\tan\beta/\tan\beta$, as a function of $\tan\beta$ based on: the rate for $e^+e^- \to b\bar{b}A + b\bar{b}H \to b\bar{b}b\bar{b}$; the rate for $e^+e^- \to HA \to b\bar{b}b\bar{b}$; and the average resolved width $\Gamma^{\rm R}_{H,A}$ defined in Eq. (7) for the H and A as determined in $e^+e^- \to HA \to b\bar{b}b\bar{b}$ events. For the rates, results for SUSY scenarios (I) and (II) differ significantly, as shown. For $b\bar{b}A + b\bar{b}H \to b\bar{b}b\bar{b}$ and $\Gamma^{\rm R}_{H,A}$ we show only the results for MSSM scenario (I). Results for scenario (II) are essentially identical. Upper and lower curves of a given type give the upper and lower 1σ bounds, respectively, obtained using a given process as shown in the figure legend. We include running b-quark mass effects and employ HDECAY [56].

upper bounds on $\tan\beta$ for $\tan\beta \gtrsim 30$. In fact, our numerical results indicate that the upper bound on $\Delta\tan\beta/\tan\beta$ decreases again as $\tan\beta$ increases beyond 30. We have traced this to the fact that HDECAY predicts that m_H decreases (at fixed $m_A = 200$ GeV) as $\tan\beta$ increases beyond 30. This results in an increase of the HA production cross section with increasing $\tan\beta$. This, in turn, implies that the $b\bar{b}b\bar{b}$ rate increases (as shown in Fig. 4) and that we can obtain an upper bound on $\tan\beta$ despite the fact that the $HA \to b\bar{b}b\bar{b}$ final state branching ratio approaches a constant value. However, since this predicted decrease of m_H at high $\tan\beta$ is somewhat peculiar to the precise parameters chosen for scenario (II), we do not regard this result as representative. For this reason, we have chosen not to show the scenario (II) upper limit curve beyond $\tan\beta = 30$. Had we plotted the region above $\tan\beta = 30$, one would see a slowly declining upper limit on $\tan\beta$.

The above results can be compared to the $\tan\beta$ determination based on the $b\bar{b}H + b\bar{b}A \to b\bar{b}b\bar{b}$ rate using the procedures of Sec. II applied in the MSSM model context. For the computation of this rate, our calculation of the $b\bar{b}H$ and $b\bar{b}A$ cross sections includes the dominant radiative corrections as incorporated via b-quark mass running starting with $m_b(m_b) = 4.62$ GeV. The H and A branching ratios and widths are computed using HDECAY. Since there is little sensitivity of this rate to the MSSM scenario (for the high $\tan\beta$ values for which this means of determining $\tan\beta$ is useful) we only present results for scenario (I); where plotted, errors for $\tan\beta$ from the $b\bar{b}H + b\bar{b}A \to b\bar{b}b\bar{b}$ rate are essentially independent of the MSSM scenario choice. The errors on $\tan\beta$ resulting from the rate for $b\bar{b}H + b\bar{b}A \to b\bar{b}b\bar{b}$ quickly become far smaller than those based on $HA \to b\bar{b}b\bar{b}$ once $\tan\beta \gtrsim 30$. This is illustrated in Fig. 5, which compares the results for $\Delta\tan\beta/\tan\beta$ obtained using the $e^+e^- \to HA \to b\bar{b}b\bar{b}$ rate to those based on the $b\bar{b}H + b\bar{b}A \to b\bar{b}b\bar{b}$ rate. This comparison shows the natural complementarity between these two techniques for measuring $\tan\beta$. However, with these two techniques alone, there is always a range of intermediate-size $\tan\beta$ values for which a good determination of $\tan\beta$ is not possible.

This "gap" can be partly filled, and the error on $\tan\beta$ at high $\tan\beta$ can be greatly reduced, by using the intrinsic total widths of the H and A to determine $\tan\beta$. However, it is only for $\tan\beta > 10$ that the intrinsic widths can provide a $\tan\beta$ determination. This is because (a) the widths are only > 5 GeV (the detector resolution discussed below) for $\tan\beta > 10$ and (b) the number of events in the $b\bar{b}b\bar{b}$ final state becomes maximal once $\tan\beta > 10$.

We now discuss the experimental issues in determining the Higgs boson width. The expected precision of the SM Higgs boson width determination at the LHC and at a LC was studied in [57]. As described in [57], a simple estimate (based on a detector energy flow resolution of $\Delta E/E = 0.3/\sqrt{E}$ for each of the two b-jets) yields an expected detector resolution of $\Gamma_{\rm res} =$ 5 GeV for $m_A \sim 200$ GeV. However, an overall fit to the $b\bar{b}$ mass distribution similar to the one in the study of [57] would give a Higgs boson resonance peak width which is about 2σ larger than that expected from the convolution of the 5 GeV resolution with the intrinsic Higgs width. This can be traced to the fact that the overall fit includes wings of the mass distribution that are present due to wrong pairings of the b-jets. The mass distribution contains about 400 di-jet masses (2 entries per HA event), of which about 300 are in a central peak. If one fits only the central peak, the width is close to that expected based on simply convoluting the 5 GeV resolution with the intrinsic Higgs width. This indicates that about 25% of the time wrong jet-pairings are made and contribute to the wings of the mass distribution. Therefore, our estimates of the error on the determination of the Higgs width will be based on the assumption that only 3/4 of the events (*i.e.* those in the central peak) retained after our basic event selection cuts (with assumed selection efficiency of 10%) can be used in the statistics computation. The $m_{b\bar{b}}$ for each of the $b\bar{b}$ pairs identified with the H or A is binned in a single mass distribution. This is appropriate since the H and A are highly degenerate for the large $\tan\beta$ values being considered so that the resolution of 5 GeV is typically substantially larger than the mass splitting. Our effective observable is then the resolved average width defined by:

$$\Gamma^{\rm R}_{H,A} = \frac{1}{2}\left[\sqrt{[\Gamma^H_{\rm tot}]^2 + [\Gamma_{\rm res}]^2} + \sqrt{[\Gamma^A_{\rm tot}]^2 + [\Gamma_{\rm res}]^2}\right] . \tag{7}$$

The resolved average width, $\Gamma^{\rm R}_{H,A}$, for SUSY scenario (I) (including $m_A = 200$ GeV) is plotted in Fig. 4 as a function of $\tan\beta$. The results for scenario (II) are indistinguishable.

In order to extract the implied $\tan\beta$ bounds, we must account for the fact that the detector resolution will not be precisely determined. There will be a certain level of systematic uncertainty which we have estimated at 10% of $\Gamma_{\rm res}$, *i.e.* $\Delta\Gamma^{\rm sys}_{\rm res} = 0.5$ GeV. This systematic uncertainty considerably weakens our ability to determine $\tan\beta$ at the lower values of $\tan\beta$ for which $\Gamma^H_{\rm tot}$ and $\Gamma^A_{\rm tot}$ are smaller than $\Gamma_{\rm res}$. This systematic uncertainty should be carefully studied as part of any eventual experimental analysis. Given $\Gamma_{\rm res}$, $\Delta\Gamma^{\rm sys}_{\rm res}$ and the number of selected $b\overline{b}b\overline{b}$ events, $N(b\overline{b}b\overline{b})$, we compute the useful number of entries in the $b\overline{b}b\overline{b}$ mass distribution for determining $\Gamma^{\rm R}_{H,A}$ as $N_{\rm entries} = 2 \times 0.75 \times N(b\overline{b}b\overline{b})$. The factor of 2 is because each $b\overline{b}b\overline{b}$ event results in two entries, one for the H and one for the A, and the factor of 0.75 is that for retaining only the central peak of the distribution. The error for $\Gamma^{\rm R}_{H,A}$ is then computed (following the procedure of [20]) as

$$\Delta\Gamma^{\rm R}_{H,A} = \left[\left(\frac{\Gamma^{\rm R}_{H,A}}{\sqrt{2N_{\rm entries}}}\right)^2 + (\Delta\Gamma^{\rm sys}_{\rm res})^2\right]^{1/2} . \tag{8}$$

The resulting upper and lower 1σ bounds on $\Gamma^{\rm R}_{H,A}$ are plotted in Fig. 4. The upper and lower limits on $\tan\beta$ are then obtained as the values $\tan\beta \pm \Delta\tan\beta$ for which the central prediction (the solid curve of Fig. 4) agrees with the values $\Gamma^{\rm R}_{H,A} \pm \Delta\Gamma^{\rm R}_{H,A}$. In computing $\Delta\Gamma^{\rm R}_{H,A}$ we have assumed a selection efficiency of 10% for computing $N(b\overline{b}b\overline{b})$. These errors are for $\mathcal{L} = 2000$ fb^{-1} and $\sqrt{s} = 500$ GeV. That an excellent determination of $\tan\beta$ will be possible at high $\tan\beta$ is apparent. The resulting accuracy for $\tan\beta$ obtained from measuring the average (resolved) H/A width is shown in Fig. 5. We see that good accuracy is already achieved for $\tan\beta$ as low as 25 with extraordinary accuracy predicted for very large $\tan\beta$. The sharp deterioration in the lower bound on $\tan\beta$ for $\tan\beta \lesssim 24$ occurs because the width falls below $\Gamma_{\rm res}$ as $\tan\beta$ is taken below the input value and sensitivity to $\tan\beta$ is lost. If there were no systematic error in $\Gamma_{\rm res}$, this sharp fall off would occur instead at $\tan\beta \lesssim 14$. To understand these effects in a bit more detail, we again give some numbers for scenario (II). At $\tan\beta = 50$, 55 and 60, $\langle\Gamma^H_{\rm tot}, \Gamma^A_{\rm tot}\rangle \sim 10.4$, 12.5 and 14.9 GeV, respectively. After including the detector resolution, the effective average widths become 11.5, 13.4 and 15.7 GeV, respectively, whereas the total error in the measurement of the average width, including systematic error, is ~ 0.54 GeV. Therefore, $\tan\beta$ can be determined to about ± 1, or to better than $\pm 2\%$. This high-$\tan\beta$ situation can be contrasted with $\tan\beta = 15$ and 20, for which $\langle\Gamma^H_{\rm tot}, \Gamma^A_{\rm tot}\rangle = 0.935$ and 1.64 GeV, respectively, which become 5.09 and 5.26 GeV after including detector resolution. Meanwhile, the total error, including the statistical error and the systematic uncertainty for $\Gamma_{\rm res}$, is about 0.57 GeV and no sensitivity to $\tan\beta$ is obtained.

The accuracies from the width measurement are somewhat better than those achieved using the $b\overline{b}A + b\overline{b}H \to b\overline{b}b\overline{b}$ rate measurement. However, both of these high-$\tan\beta$ methods for determining $\tan\beta$ are important because they are beautifully complementary in that they rely on very different experimental observables. Further, both methods are nicely complementary in their $\tan\beta$ coverage to the $\tan\beta$ determination based on the $HA \to b\overline{b}b\overline{b}$ rate, which comes in at lower $\tan\beta$. In fact, the width measurement can provide a decent $\tan\beta$ determination even in the previously identified "gap" region where neither the $HA \to b\bar{b}b\bar{b}$ nor the $b\bar{b}A + b\bar{b}H \to b\bar{b}b\bar{b}$ rates were able to provide such a determination. In particular, in the case of MSSM scenario (II), combining the $HA \to b\bar{b}b\bar{b}$ rate and the width measurements implies that the worst $\tan\beta$ lower bound is $\Delta\tan\beta/\tan\beta \sim -0.25$ at $\tan\beta \sim 28$ and the worst $\tan\beta$ upper bound is $\Delta\tan\beta/\tan\beta \sim +0.30$ at $\tan\beta \sim 20$. However, in the case of MSSM scenario (I) a good upper bound on $\tan\beta$ is not possible if $\tan\beta \sim 12-15$, even after including the width measurement. Overall, there is a window, $10 \lesssim \tan\beta \lesssim 25$ in scenario (I) or $20 \lesssim \tan\beta \lesssim 25$ in scenario (II), for which an accurate determination of $\tan\beta$ ($\Delta\tan\beta/\tan\beta < 0.2$) using just the $b\bar{b}b\bar{b}$ final state processes will not be possible. This window expands rapidly as m_A increases (keeping $\sqrt{s}$ fixed). Indeed, as m_A increases above 250 GeV, HA pair production becomes kinematically forbidden at $\sqrt{s} = 500$ GeV and, in addition, detection of the $b\bar{b}H + b\bar{b}A$ processes at the LC (or the LHC) requires [58] increasingly large values of $\tan\beta$. This difficulty persists even for $\sqrt{s} \sim 1$ TeV and above; if $m_A > \sqrt{s}/2$, the H and A cannot be pair-produced and yet the rate for $b\bar{b}H + b\bar{b}A$ production is undetectably small for moderate $\tan\beta$ values.

In the above study, we have not made use of other decay channels of the H and A, such as $H \to WW, ZZ$, $H \to hh$, $A \to Zh$ and $H, A \to$ SUSY. The theoretical studies of [33, 34] indicate that their inclusion could improve the precision with which $\tan\beta$ is measured at low to moderate $\tan\beta$ values. A determination of $\Gamma^{\rm R}_{H,A}$ is also possible using the $b\bar{b}A + b\bar{b}H \to b\bar{b}b\bar{b}$ events. To estimate how well $\tan\beta$ can be determined in this way, let us assume that 50% of the events selected in the analysis of Sec. II can be used for a fit of the average width and that (as in the $HA \to b\bar{b}b\bar{b}$ study) a resolution of 5 GeV can be achieved, based on a detector energy flow resolution of $\Delta E/E = 0.3/\sqrt{E}$. If we again assume that 10% systematic error for the width measurement can be achieved, the resulting $\tan\beta$ errors would be similar to those obtained from the $b\bar{b}A + b\bar{b}H \to b\bar{b}b\bar{b}$ event rate for $\tan\beta > 30$ (see Fig. 5), *i.e.* not as small as the $\tan\beta$ errors obtained from the measurement of $\Gamma^{\rm R}_{H,A}$ in $HA \to b\bar{b}b\bar{b}$ events. A complete analysis that takes into account the significant background and the broad energy spectrum of the radiated H and A is needed to reliably assess the $\tan\beta$ errors that would be obtained by measuring $\Gamma^{\rm R}_{H,A}$ in $b\bar{b}A + b\bar{b}H \to b\bar{b}b\bar{b}$ events. If $\tan\beta$ is large enough, $b\bar{b}A + b\bar{b}H \to b\bar{b}b\bar{b}$ would be observable in the MSSM even when $m_A > \sqrt{s}/2$, or, for a more general model, whenever HA pair production is kinematically forbidden but $b\bar{b}A \to b\bar{b}b\bar{b}$ and/or $b\bar{b}H \to b\bar{b}b\bar{b}$ production is allowed. Then, the event rate for, and width measurements from $b\bar{b}A$ and/or $b\bar{b}H$ production would allow a determination of $\tan\beta$. We have not attempted a quantitative study of this situation.

Let us briefly return to the interpretation of these measurements in terms of $\tan\beta$. As stated in the introduction, we are using $\tan\beta$ as a tree-level mnemonic to characterize the $b\bar{b}$ Yukawa coupling of the Higgs bosons. For the soft-SUSY-breaking parameters for MSSM scenarios (I) and (II), the one-loop corrections to the $b\bar{b}$ couplings of the H and A and the stop/sbottom mixing present in the one-loop corrections to the Higgs mass matrix [53] are small. More generally, however, substantial ambiguity can arise, especially if the sign and magnitude of μ is not fixed. Assuming that these parameters are known, the errors for the Yukawa coupling obtained from these measurements can be related to any given definition of $\tan\beta$ and, except in very unusual cases, the resulting error on $\tan\beta$ would be fairly insensitive to the precise scenario. For example, one possible definition of $\tan\beta$ would be that the $\mu^+\mu^- A$ coupling should be precisely given by $-(m_b/v)\tan\beta$, see Eq (4). This is a convenient definition since the $\mu^+\mu^- A$ coupling will have very modest higher-order corrections relative to the tree-level and any such corrections can then be sensibly absorbed using the above definition of $\tan\beta$. Given this definition of $\tan\beta$, the $Hb\bar{b}$ and $Ab\bar{b}$ couplings can be computed to any desired order once the necessary MSSM parameters are known. In this way, all the probes of heavy Higgs Yukawa couplings discussed in this paper can be related to this common definition of $\tan\beta$.

For larger Higgs boson masses above 200 GeV, higher center-of-mass energies of a e^+e^- collider would be a necessary to study their properties and to measure $\tan\beta$. In fact the increase of the center-of-mass energy in a second phase of a Linear Collider operation is foreseen. For center-of-mass energies below 200 GeV and above the current experimental limit of about 90 GeV, expected event rates would increase mostly in the $b\bar{b}A$ analysis and would lead to higher sensitivity. Figure 3 gives a comparison of the variation of the $\tan\beta$ sensitivity for $m_A = 100, 150, 200$ GeV.

IV H^+H^- PRODUCTION: DECAY BRANCHING RATIOS AND TOTAL WIDTH

In this section, we extend our study to include charged Higgs boson production processes. Existing analyses of $e^+e^- \to H^+H^-$ production indicate that the absolute event rates and ratios of branching ratios in various H^+H^- final state channels will allow a relatively accurate determination of $\tan\beta$ at low $\tan\beta$ [33, 34]. The process $e^+e^- \to H^\pm tb$ can also be sensitive to $\tan\beta$ [35]. Here, we focus on an experimentally based analysis of the determination of $\tan\beta$ using the $H^+H^- \to t\bar{b}\bar{t}b$ event rate. As anticipated on the basis of the earlier work referenced above, we find that good accuracy can be achieved at low $\tan\beta$. We also demonstrate that the total width of the $H^\pm$ measured in the tb decay channel using $H^+H^- \to t\bar{b}\bar{t}b$ production will allow a fairly precise determination of $\tan\beta$ at high $\tan\beta$. Since these two techniques for determining $\tan\beta$ are statistically independent of one another and of the $\tan\beta$ measurements that employ neutral Higgs production, they will increase the overall accuracy with which $\tan\beta$ can be measured at both low and high $\tan\beta$.

The reaction $e^+e^- \to H^+H^- \to t\bar{b}\bar{t}b$ can be observed at a LC [59], and recent high-luminosity simulations [60] show that the cross section times branching ratio can be measured precisely. As soon as the charged Higgs boson decay into tb is allowed this decay mode is dominant. Nonetheless, BR($H^\pm \to tb$) varies significantly with $\tan\beta$, especially for small values of $\tan\beta$ where the tb mode competes with the $\tau\nu$ mode. The $H^+ \to t\bar{b}$ branching ratio and width are sensitive to $\tan\beta$ in the form

$$\Gamma(H^\pm \to tb) \propto m_t^2 \cot^2\beta + m_b^2 \tan^2\beta\,. \tag{9}$$

As in Sec. III, we will use HDECAY (which incorporates running of the b-quark mass) to evaluate the charged Higgs boson branching ratios and decay width. It is useful to note that the above form results in a minimum in the tb partial width and branching ratio in the vicinity of $\tan\beta \sim 6-8$. The depth of the minimum in the branching ratio depends upon the extent to which the tb channel is competing against other modes. In contrast, the cross section for $e^+e^- \to H^+H^-$ production is independent of $\tan\beta$ at tree-level. (The one-loop corrections [61] result in a 10% variation of the cross section with $\tan\beta$ which must be taken into account when the data are taken; we do not include them in our study.) The net result is that the rate for $e^+e^- \to H^+H^- \to t\bar{b}\bar{t}b$ has significant dependence upon $\tan\beta$, coming mainly from the variation in the branching ratio.

Our procedures for estimating errors for the $t\bar{b}\bar{t}b$ rate and for the total width are similar to those given earlier for HA production rates and width in the $b\bar{b}b\bar{b}$ channel. We base our

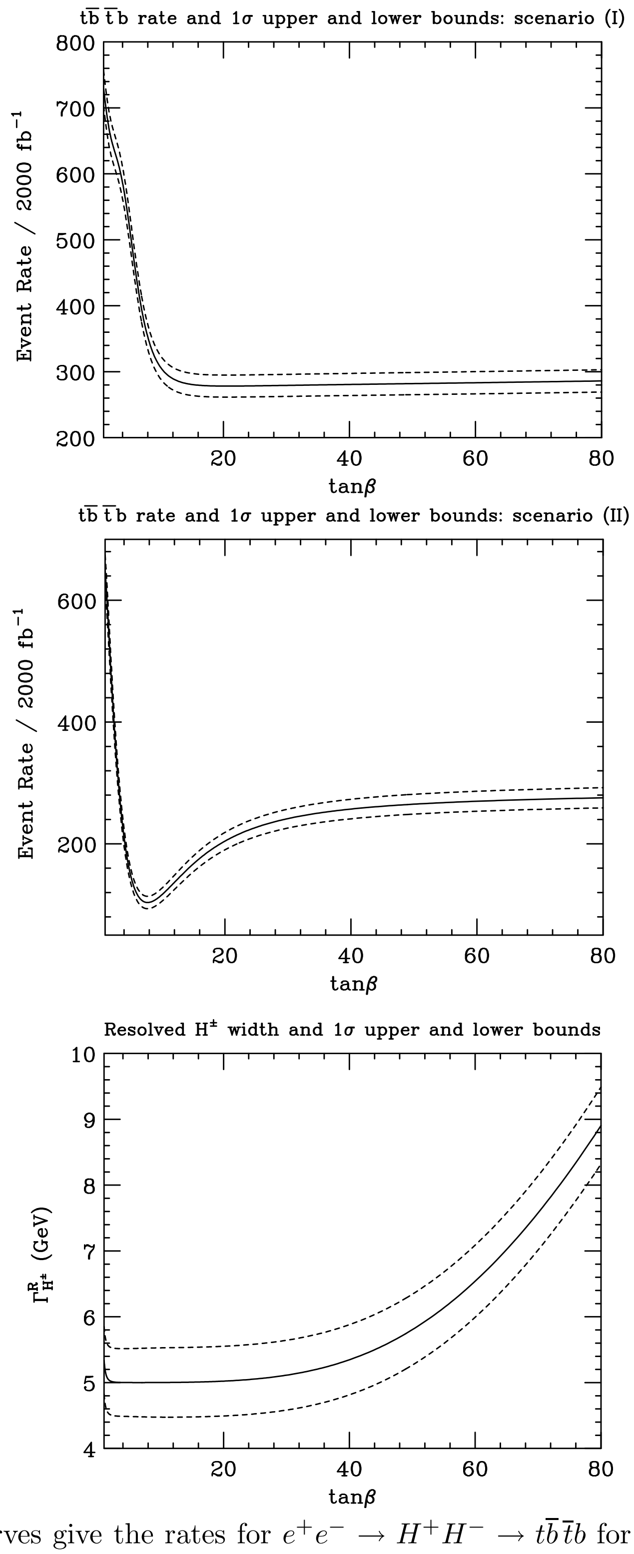

FIG. 6: The solid curves give the rates for $e^+e^- \to H^+H^- \to t\bar{b}\bar{t}b$ for MSSM scenarios (I) and (II) in the upper two figures and $\Gamma^{\rm R}_{H^\pm}$, Eq. (10), for scenario (I) in the lower figure. The dashed curves are the corresponding 1σ upper and lower bounds. We take $m_{H^\pm} = 200$ GeV, $\sqrt{s} = 500$ GeV and $\mathcal{L} = 2000$ fb^{-1}. An efficiency of 2.2% is assumed for cuts, acceptance and tagging. The upper and lower 1σ bounds for $\Gamma^{\rm R}_{H^\pm}$ include an additional efficiency factor of 0.75 (which corresponds to keeping only events in the central mass peak) and assume the estimated mass resolution of $\Gamma_{\rm res} = 5$ GeV, including 10% systematic uncertainty. The $\Gamma^{\rm R}_{H^\pm}$ results obtained in scenario (II) are very similar to those plotted for scenario (I).

efficiency for the $t\bar{b}\,\bar{t}b$ final state on the study of [60]. For $m_{H^\pm} = 300$ GeV at $\sqrt{s} = 800$ GeV, this study finds that the $t\bar{b}\,\bar{t}b$ final state can be isolated with an efficiency of 2.2%. The reason for the much lower efficiency as compared to 10% efficiency for the $b\bar{b}b\bar{b}$ final state of HA production is the difficulty of assigning the non-b jets from t-decays to the correct top mass cluster. For $\sqrt{s} = 500$ GeV and $m_{H^\pm} = 200$ GeV, we have adopted the same 2.2% efficiency, for which we assume little or no background after cuts. For the total width determination, we assume that we keep only 75% of the events after cuts (*i.e.* a fraction 0.75×0.022 of the raw event number), corresponding to throwing away wings to the mass peaks, and each $t\bar{b}\,\bar{t}b$ event is counted twice since we can look at both the H^+ and the H^- decay. We define a resolved width which incorporates the intrinsic resolution for the width determination, taken to be $\Gamma_{\rm res} = 5$ GeV:

$$\Gamma^{\rm R}_{H^\pm} = \sqrt{[\Gamma^{H^\pm}_{\rm tot}]^2 + [\Gamma_{\rm res}]^2}\,. \tag{10}$$

Estimated errors based on the width measurement will assume a 10% systematic error in our knowledge of $\Gamma_{\rm res}$, *i.e.* $\Delta\Gamma^{\rm sys}_{\rm res} = 0.5$ GeV as for the H, A case. We employ Eq. (8), with the replacement $\Gamma^{\rm R}_{H,A} \to \Gamma^{\rm R}_{H^\pm}$, to compute $\Delta\Gamma^{\rm R}_{H^\pm}$. In this case, $N_{\rm entries} = 2 \times 0.75 \times N(t\bar{b}\,\bar{t}b)$, where $N(t\bar{b}\,\bar{t}b)$ is computed using the above-noted selection efficiency of 0.022. Figure 6 shows the resulting $t\bar{b}\,\bar{t}b$ final state rate, $N(t\bar{b}\,\bar{t}b)$, for MSSM scenarios (I) and (II) and the resolved width ($\Gamma^{\rm R}_{H^\pm}$) for scenario (I). Also shown are the corresponding 1σ upper and lower bounds on the rate and resolved width. These are then used in exactly the same manner as described in the HA case to determine the upper and lower bounds on $\tan\beta$.

For the rate, we observe from Fig. 6 that upper bounds on $\tan\beta$ will be poor once $\tan\beta \gtrsim 10$ because of the very slow variation of the $t\bar{b}\,\bar{t}b$ final rate in this region. At high $\tan\beta$, for SUSY scenario (I) lower bounds will be determined by the part of the $t\bar{b}\,\bar{t}b$ rate curve that rises rapidly when $\tan\beta$ falls below 10. For SUSY scenario (II), the beginning of the dip will fix the lower bounds on $\tan\beta$ when $\tan\beta$ is large, assuming that we know ahead of time from other experimental data that $\tan\beta$ is larger than 15. As regards the width, the main point to note is that $\Gamma^{\rm tot}_{H^\pm}$ rises only slowly with increasing $\tan\beta$. As a result, the 5 GeV resolution and 10% systematic error for this resolution are significant compared to the < 10 GeV $H^\pm$ width that applies throughout the $\tan\beta$ range studied. Note also, that for moderate $\tan\beta$ values, there will be no lower bound on $\tan\beta$ as a result of the fact that $\Gamma^{\rm R}_{H^\pm}$ never falls below $\Gamma_{\rm res} = 5$ GeV, while the 1σ errors are substantially lower than this. We will also assume that if $\tan\beta$ is large, then we will know from other experimental information (such as the HA final state) that $\tan\beta$ is not small and that the small rise in the width for $\tan\beta \sim 1$ is not relevant.

The resulting $\tan\beta$ upper and lower bounds appear in Fig. 7. Comparing to Fig. 5, we observe that for SUSY scenario (I) the $t\bar{b}\,\bar{t}b$ rate measurement gives a $\tan\beta$ determination that is quite competitive with that from HA production in the $b\bar{b}b\bar{b}$ final state. For SUSY scenario (II), the $t\bar{b}\,\bar{t}b$ rate gives an even better $\tan\beta$ determination than does the $b\bar{b}b\bar{b}$ rate. On the other hand, the width measurement from the $t\bar{b}\,\bar{t}b$ final state of H^+H^- production is much poorer than that from the $b\bar{b}b\bar{b}$ final state of HA production, as was to be expected from the discussion given earlier.

The rate for $e^+e^- \to t\bar{b}H^- + \bar{t}bH^+ \to t\bar{t}b\bar{b}$ is also very sensitive to $\tan\beta$ and might be a valuable addition to the $e^+e^- \to H^+H^- \to t\bar{b}\,\bar{t}b$ and $e^+e^- \to b\bar{b}A + b\bar{b}H \to b\bar{b}b\bar{b}$ rate determinations of $\tan\beta$. The theoretical study of [35] finds, for example, that if $m_{H^\pm} = 200$ GeV and $\tan\beta = 50$ ($\tan\beta = 20$), then the 1σ errors (including systematic uncertainties) on $\tan\beta$ are $\Delta\tan\beta/\tan\beta = 0.06$ ($\Delta\tan\beta/\tan\beta = 0.2$), respectively, for $\mathcal{L} = 2000$ fb^{-1} and $\sqrt{s} = 500$ GeV.

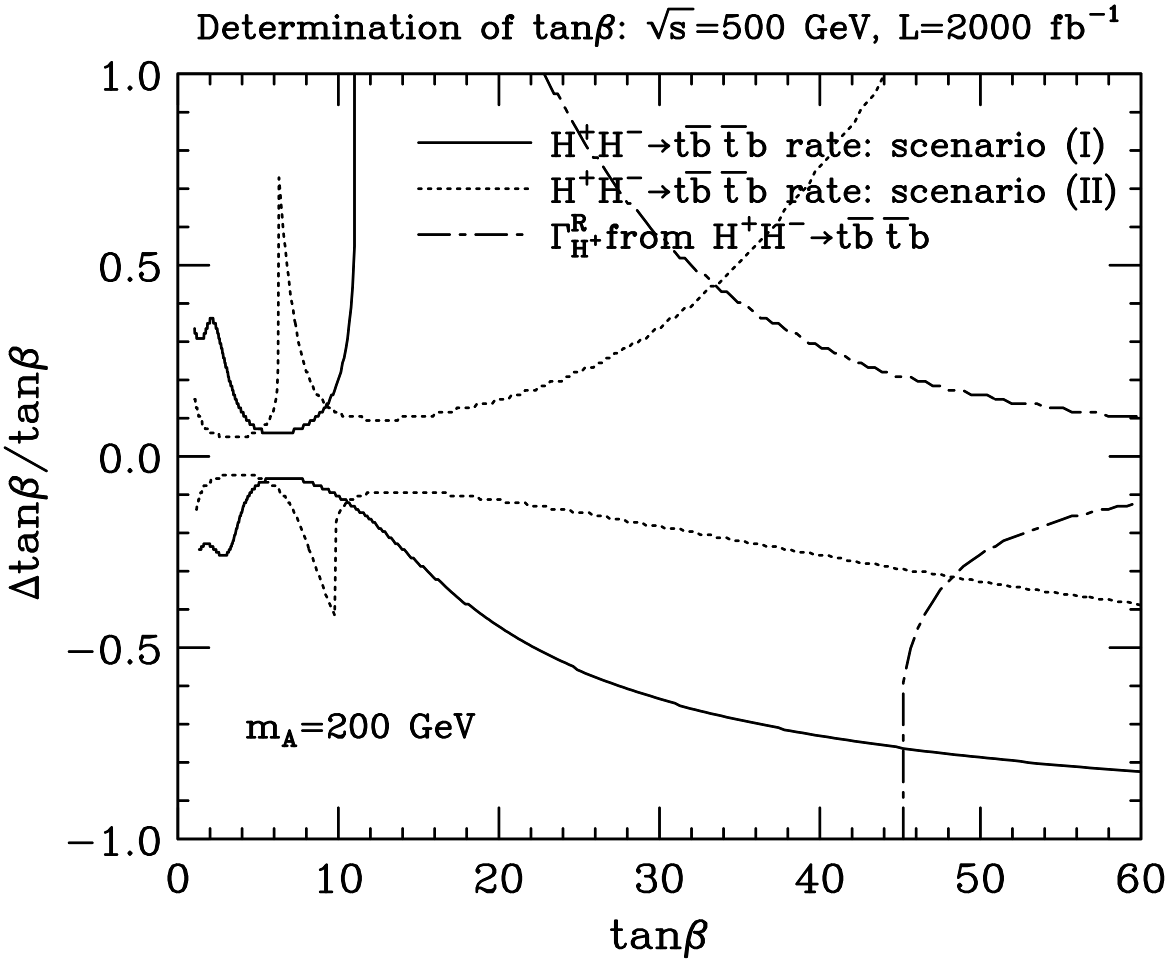

FIG. 7: For the MSSM with $m_{H^\pm} \sim m_A = 200$ GeV, and assuming $\mathcal{L} = 2000$ fb^{-1} at $\sqrt{s} = 500$ GeV, we plot the 1σ statistical upper and lower bounds, $\Delta \tan\beta/\tan\beta$, as a function of $\tan\beta$ based on: the rate for $e^+e^- \to H^+H^- \to t\bar{b}\bar{t}b$; and the resolved width $\Gamma^{\rm R}_{H^\pm}$ defined in Eq. (10) as determined in $e^+e^- \to H^+H^- \to t\bar{b}\bar{t}b$ events. For the rates, results for SUSY scenarios (I) and (II) differ significantly, as shown. For $\Gamma^{\rm R}_{H^\pm}$ we show only the results for MSSM scenario (I). Results for scenario (II) are essentially identical. Upper and lower curves of a given type give the upper and lower 1σ bounds, respectively, obtained using a given process as shown in the figure legend. We include running b-quark mass effects and employ HDECAY [56].

By combining in quadrature the $\tan\beta$ errors for the various individual measurements, as given in Figs. 5 and 7, we obtain the net errors on $\tan\beta$ shown in Fig. 8. The influence on the $\tan\beta$ determination of the precise SUSY scenario is large in the intermediate $\tan\beta$ region, as shown in Fig. 8. Scenario I and II are chosen to illustrate the dependence on the possibility that the Higgs bosons can decay into SUSY particles. We therefore stress the importance of measuring the light SUSY particle spectrum before $\tan\beta$ can be determined with precision.

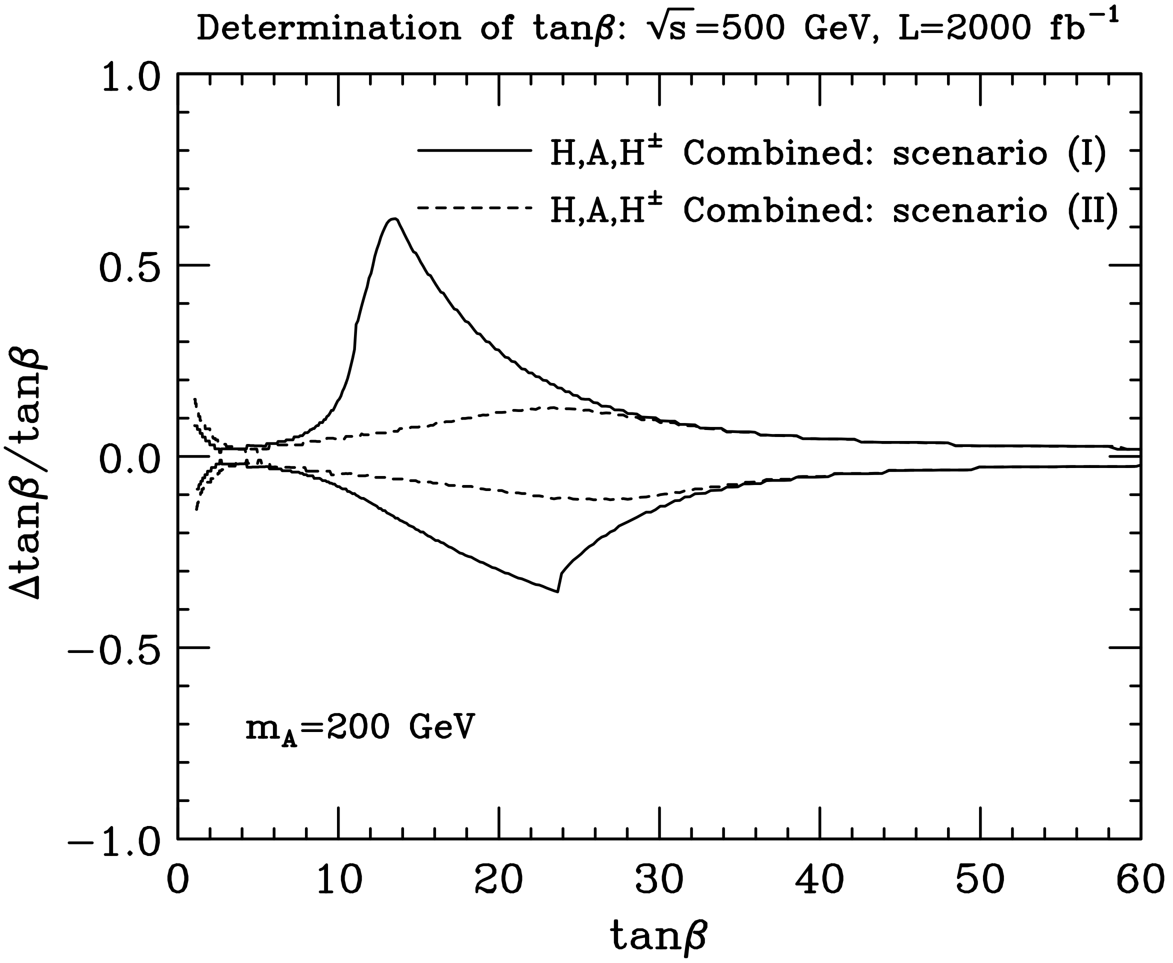

FIG. 8: For the MSSM with $m_{H^\pm} \sim m_A = 200$ GeV, and assuming $\mathcal{L} = 2000$ fb^{-1} at $\sqrt{s} = 500$ GeV, we plot the 1σ statistical upper and lower bounds, $\Delta \tan\beta/\tan\beta$, as a function of $\tan\beta$ based on combining (in quadrature) the results shown in Figs. 5 and 7. Results are shown for the SUSY scenarios (I) and (II) described in the text.

V COMPARISON TO LHC DETERMINATIONS OF $\tan\beta$

In this section, we will compare the LC results summarized in Figs. 5, 7 and 8 to the $\tan\beta$ accuracies that can be achieved at the LHC based on $H, A, H^\pm$ production and decay processes. First note that there is a wedge-shaped window of moderate $\tan\beta$ and $m_A \gtrsim 200$ GeV for which the A, H and $H^\pm$ are all unobservable (see, for example, Refs. [21, 22, 62]). In this wedge, the only Higgs boson that is detectable at the LHC is the light SM-like Higgs boson, h. Precision measurements of the properties of the h typically only provide weak sensitivity to $\tan\beta$, and will not be considered here. The lower $\tan\beta$ bound of this moderate-$\tan\beta$ wedge is defined by the LEP-2 limits [9], which are at $\tan\beta \sim 3$ for $m_A \sim 200$ GeV, falling to $\tan\beta \sim 2.5$ for $m_A \gtrsim 250$ GeV, assuming the maximal mixing scenario [see SUSY scenario (I) defined earlier]. The upper $\tan\beta$ limit of the wedge is at $\tan\beta \sim 7$ for $m_A \sim 200$ GeV rising to $\tan\beta \sim 15$ at $m_A \sim 500$ GeV. For either smaller or larger $\tan\beta$ values, the heavy MSSM Higgs bosons can be detected and their production rates and properties will provide sensitivity to $\tan\beta$.

We will now summarize the results currently available regarding the determination of $\tan\beta$ at the LHC using Higgs measurements (outside the wedge region) assuming a luminosity of $\mathcal{L} = 300$ fb^{-1}. The methods employed are those proposed in [20]. The reactions that have been studied at the LHC are the following.

1. $H \to ZZ \to 4\ell$ [22].

   The best accuracy that can be achieved at low $\tan\beta$ is obtained from the $H \to ZZ \to 4\ell$ rate. One finds $\Delta\tan\beta/\tan\beta = \pm 0.1$ at $\tan\beta = 1$ rising to $> \pm 0.3$ by $\tan\beta = 1.5$ for the sample choice of $m_H = 300$ GeV. For $m_H < 2m_Z$, $\tan\beta$ cannot be measured via this process. In the MSSM maximal mixing scenario, such low values of $\tan\beta$ are unlikely in light of LEP-2 results.

2. $gg \to H + gg \to A \to \tau^+\tau^-, \mu^+\mu^-$ and $gg \to b\bar{b}H + b\bar{b}A \to b\bar{b}\tau^+\tau^-, b\bar{b}\mu^+\mu^-$ [22].

   At high $\tan\beta$ and taking $m_A = 150$ GeV, Fig. 19-86 of [22] shows that the $gg \to H \to \tau^+\tau^-$, $gg \to A \to \tau^+\tau^-$, and $gg \to b\bar{b}A + b\bar{b}H \to b\bar{b}\tau^+\tau^-$ rates can, in combination, be used to determine $\tan\beta$ with an accuracy of ± 0.15 at $\tan\beta = 5$, improving to ± 0.06 at $\tan\beta = 40$. The corresponding rates with $H, A \to \mu^+\mu^-$ yield a somewhat better determination at higher $\tan\beta$: ± 0.12 at $\tan\beta = 10$ and ± 0.05 at $\tan\beta = 40$.

   Interpolating, using Figs. 19-86 and 19-87 from [22], we estimate that at $m_A \sim 200$ GeV (our choice for this study) the error on $\tan\beta$ based on these rates would be smaller than ± 0.1 for $\tan\beta \gtrsim 13$, asymptoting to ± 0.05 at large $\tan\beta$.

   It is important to note that the $\tan\beta$ sensitivity for $\tan\beta < 20 - 30$ is largely due to the loop-induced $gg \to A$ and $gg \to H$ production processes. Thus, interpreting these fully inclusive rates in terms of $\tan\beta$ when $\tan\beta < 20 - 30$ requires significant knowledge of the particles, including SUSY particles, that go into the loops responsible for the $gg \to H$ and $gg \to A$ couplings.

   The importance of including the $gg \to H$, $gg \to A$ as well as the $gg \to b\bar{b}H + gg \to b\bar{b}A$ processes in order to obtain observable signals for $\tan\beta$ values as low as 10 in the $\mu^+\mu^-$ channels is apparent from [63]. For $\mathcal{L} = 300$ fb^{-1} and $m_A = 200$ GeV, they find that the $b\bar{b}\mu^+\mu^-$ final states can only be isolated for $\tan\beta > 30$ whereas the inclusive $\mu^+\mu^-$ final state from all production processes becomes detectable once $\tan\beta > 10$.

3. $gg \to t\bar{b}H^- + \bar{t}bH^+$ with $H^\pm \to \tau^\pm\nu$ [24].

   The $tbH^\pm \to tb\tau\nu$ rate gives a fractional $\tan\beta$ uncertainty, $\Delta\tan\beta/\tan\beta$, ranging from ± 0.074 at $\tan\beta = 20$ to ± 0.054 at $\tan\beta = 50$. This signal is somewhat cleaner to interpret in terms of a $\tan\beta$ measurement than the inclusive signals for the H and A summarized above, since there are no uncertainties related to SUSY loop contributions.

Sensitivity to $\tan\beta$ deriving from direct measurements of the decay widths has not been studied by the LHC experiments. One can expect excellent $\tan\beta$ accuracy at the higher $\tan\beta$ values for which the $gg \to b\bar{b}\mu^+\mu^-$ signal for the H and A is detectable.

Let us now compare these LHC results to the LC errors for $\tan\beta$, assuming $m_A = 200$ GeV. First, consider $\tan\beta \leq 10$. As summarized above, the LHC error on $\tan\beta$ is ± 0.12 at $\tan\beta \sim 10$ and at $\tan\beta \sim 1$, and the error becomes very large for $1.5 \lesssim \tan\beta \lesssim 5$. Meanwhile, the LC error from Fig. 8 ranges from roughly ± 0.03 to ± 0.05 for $2 \lesssim \tan\beta \lesssim 5$ rising to about ± 0.1 at $\tan\beta \sim 10$ [in the less favorable SUSY scenario (I)]. Therefore, for $\tan\beta \lesssim 10$ the

LC provides the best determination of $\tan\beta$ using Higgs observables related to their Yukawa couplings. (In the MSSM context, other non-Higgs LHC measurements would allow a good $\tan\beta$ determination at low to moderate $\tan\beta$ based on other kinds of couplings.) In the middle range of $\tan\beta$ (roughly $13 < \tan\beta < 30$ at $m_A \sim 200$ GeV), the heavy Higgs determination of $\tan\beta$ at the LHC might be superior to that obtained at the LC. This depends upon the SUSY scenario: if the heavy Higgs bosons can decay to SUSY particles, the LC will give $\tan\beta$ errors that are quite similar to those obtained at the LHC; if the heavy Higgs bosons do not have substantial SUSY decays, then the expected LC $\tan\beta$ errors are substantially larger than those predicted for the LHC. At large $\tan\beta$, the LC measurement of the heavy Higgs couplings and the resulting $\tan\beta$ determination at the LC is numerically only slightly more accurate than that obtained at the LHC. For example, both are of order ± 0.05 at $\tan\beta = 40$. These comparisons are summarized in Table I. It is possible that the net LHC $\tan\beta$ error would be somewhat smaller than the LC error for $\tan\beta \gtrsim 40$ if both ATLAS and CMS can each accumulate $\mathcal{L} = 300$ fb^{-1} of luminosity; combining the two data sets would presumably roughly double the statistics and decrease errors by a factor of order $1/\sqrt{2}$. In any case, a very small error on $\tan\beta$ will be achievable for all $\tan\beta$ by combining the results from the LC with those from the LHC. [65]

VI CONCLUSIONS

A high-luminosity linear collider will provide a precise determination of the value of $\tan\beta$ throughout much of the large range of possible interest, $1 < \tan\beta < 60$. In this paper, we have studied the sensitivity to $\tan\beta$ that will result from measurements of heavy Higgs boson production processes, branching fractions and decay widths. These are all directly determined by the ratio of vacuum expectation values that defines $\tan\beta$, and each can be very accurately measured at an LC over a substantial range of relevant $\tan\beta$ values. In particular, there are

TABLE I: A comparison of fractional errors, $\Delta\tan\beta/\tan\beta$, achievable for $\mathcal{L} = 2000$ fb^{-1} at the LC with those expected at the LHC for $\mathcal{L} = 300$ fb^{-1}, assuming $m_A = 200$ GeV in the MSSM. LC results are given for both SUSY scenarios (I) and (II), where Higgs boson decays to SUSY particles are disallowed, respectively allowed. LHC results are estimated by roughly combining the determinations of $\tan\beta$ based on H, A production from [22] with those using $H^\pm$ production from [24], both of which assume the standard MSSM maximal mixing scenario. All entries are approximate.

$\tan\beta$ range	LHC	LC (case I)	LC (case II)
1	0.12	0.15	0.1
1.5–5	very large	0.03–0.05	0.03–0.05
10	0.12	0.1	0.05
13–30	0.05	0.6–0.1	0.05–0.1
40–60	0.05–0.03	0.05–0.025	0.05–0.025

several Higgs boson observables which are likely to provide the most precise measurement of $\tan\beta$ when $\tan\beta$ is very large. In the context of the MSSM, there is a particularly large variety of complementary methods that will allow an accurate determination of $\tan\beta$ when $m_A \lesssim \sqrt{s}/2$ so that $e^+e^- \to HA$ pair production is kinematically allowed. Using the sample case of $m_A = 200$ GeV (in the MSSM context) and a LC with $\sqrt{s} = 500$ GeV, we have demonstrated the complementarity of employing:

a) the $b\overline{b}A$, $b\overline{b}H \to b\overline{b}b\overline{b}$ rate;

b) the $HA \to b\overline{b}b\overline{b}$ rate;

c) a measurement of the average H, A total width in HA production;

d) the $H^+H^- \to t\overline{b}\,\overline{t}b$ rate; and

e) the total $H^\pm$ width measured in $H^+H^- \to t\overline{b}\,\overline{t}b$ production.

By combining the $\tan\beta$ errors from all these processes in quadrature, we obtain the net errors on $\tan\beta$ shown in Fig. 8 by the lines [solid for SUSY scenario (I) and dashed for SUSY scenario (II)], assuming a multi-year integrated luminosity of $\mathcal{L} = 2000$ fb^{-1}. We see that, independent of the scenario, the Higgs sector will provide an excellent determination of $\tan\beta$ at small and large $\tan\beta$ values, leading to an error on $\tan\beta$ of 10% or better. If SUSY decays of the $H, A, H^\pm$ are significant [SUSY scenario (II)], the $\tan\beta$ error will be smaller than 13% even in the more difficult moderate $\tan\beta$ range. However, if SUSY decays are not significant [SUSY scenario (I)] there is a limited range of moderate $\tan\beta$ for which the error on $\tan\beta$ would be large, reaching about 50%.

In the preceding section, we considered how these $\tan\beta$ errors from the LC compared to $\tan\beta$ errors determined at the LHC based only on measurements involving $H, A, H^\pm$ production and decay. The broad conclusions were: (i) for low $\tan\beta$ ($\lesssim 10$) the errors on $\tan\beta$ from LHC Higgs measurements would be much larger than those attainable at the LC; (ii) for high $\tan\beta$ ($\gtrsim 30$) the LHC and LC $\tan\beta$ errors were both small and quite comparable in magnitude; and (iii) in the moderate-$\tan\beta$ range ($13 \lesssim \tan\beta \lesssim 30$) the LHC errors on $\tan\beta$ would very possibly be smaller than the LC errors. However, we also noted that in this latter region some care in interpretation of the LHC results would be necessary due to the need to include loop-induced $gg \to H$ and $gg \to H$ production processes in order to obtain good sensitivity to $\tan\beta$; these might be influenced by loops of SUSY particles and, possibly, other undiscovered new physics. This LHC versus LC comparison should also be viewed as highly preliminary since the LHC collaborations have not yet studied all the relevant observables. In particular, they have not looked at the $\tan\beta$ determination using the directly measured widths of the H and A. Regardless of the relative magnitude of the LHC versus LC $\tan\beta$ errors, the clean LC environment will provide an important and independent measurement that will complement any LHC determination of $\tan\beta$. Different uncertainties will be associated with the determination of $\tan\beta$ at a hadron and an e^+e^- collider because of the different backgrounds. Further, the LHC and LC measurements of $\tan\beta$ will be highly complementary in that the systematic errors involved will be very different.

Combining all the different LC measurements as above does not fully account for the fact that the "effective" $\tan\beta$ value being measured in each process is only the same at tree-level. The $\tan\beta$ values measured via the $H \to b\overline{b}$ Yukawa coupling, the $A \to b\overline{b}$ Yukawa coupling and the $H^+ \to t\overline{b}$ Yukawa coupling could all be influenced differently by the MSSM one-loop corrections. For some choices of MSSM parameters, the impact of MSSM radiative corrections on interpreting these measurements can be substantial [53]. However, if the masses of the SUSY particles are known, so that the important MSSM parameters entering these radiative corrections (other than $\tan\beta$) are fairly well determined, then a uniform convention for the definition of $\tan\beta$ can be adopted and, in general, an excellent determination of $\tan\beta$ (with accuracy similar to that obtained via our tree-level procedures) will be possible using the linear collider observables considered here. Even for special SUSY parameter choices such that one of the Yukawa couplings happens to be significantly suppressed, the observables a)-e) would provide an excellent opportunity for pinning down all the Yukawa couplings and checking the consistency of the MSSM model.

Finally, it is important to note that the techniques considered here can also be employed in the case of other Higgs sector models. For example, in the general (non-SUSY) 2HDM, if the only non-SM-like Higgs boson with mass below $\sqrt{s}$ is the A [64], then a good determination of $\tan\beta$ will be possible at high $\tan\beta$ from the $b\overline{b}A \to b\overline{b}b\overline{b}$ production rate. Similarly, in models with more than two Higgs doublet and/or triplet representations, the Yukawa couplings of the Higgs bosons, and, therefore, the analogues of the 2HDM parameter $\tan\beta$, will probably be accurately determined through Higgs production observables in e^+e^- collisions.

Acknowledgments

We wish to thank Ron Settles for discussions regarding the expected detector resolution. This work was supported in part by the U.S. Department of Energy under grants DE-FG02-95ER40896, DE-FG03-91ER40674, and W-31109-ENG-38, and in part by the Davis Institute for High Energy Physics, the Wisconsin Alumni Research Foundation, and the Particle Physics and Astronomy Research Council, UK.

REFERENCES

References

[1] J.F. Gunion, H.E. Haber, G. Kane and S. Dawson, *The Higgs Hunter's Guide* (Addison-Wesley, Redwood City, California, 1990).

[2] J.F. Gunion and H.E. Haber, Nucl. Phys. B **272**, 1 (1986), ERRATUM-ibid. B **402**, 567 (1993).

[3] H.E. Haber and Y. Nir, Nucl. Phys. B **335**, 363 (1990).

[4] J. F. Gunion and H. E. Haber, arXiv:hep-ph/0207010.

[5] V. Barger, M. S. Berger and P. Ohmann, Phys. Rev. D **47**, 1093 (1993), D **49**, 4908 (1994); M. Carena, S. Pokorski and C.E.M. Wagner, Nucl. Phys. B **406**, 59 (1993).

[6] B. Ananthanarayan, G. Lazarides and Q. Shafi, Phys. Rev. D **44**, 1613 (1991); L. J. Hall, R. Rattazzi and U. Sarid, Phys. Rev. D **50**, 7048 (1994); L.J. Hall and S. Raby, Phys. Rev. D **51**, 6524 (1995).

[7] H. Haber and R. Hempfling, Phys. Rev. Lett. **66**, 1815 (1991); M. Carena, P.H. Chankowski, S. Pokorski and C. Wagner, Phys. Lett. B **411**, 205 (1998); S. Heinemeyer, W. Hollik and G. Weiglein, Phys. Rev. D **58**, 091701 (1998); Phys. Lett. B **440**, 296 (1998); R.-J. Zhang, Phys. Lett. B **447**, 89 (1998); J.R. Espinosa and R.-J. Zhang [arXiv:hep-ph/0003246].

[8] A. Sopczak, Phys. Rep. **359**, 169 (2002).

[9] LEP Higgs Working Group, July 2002.

[10] A. Sopczak, *Nucl. Phys. B (Proc. Suppl.)* B **109**, 271 (2002).

[11] For a recent summary, see *e.g.*, L. Moneta [CDF collaboration], arXiv:hep-ex/0106050, in the proceedings of *36th Rencontres de Moriond on QCD and Hadronic Interactions*, Les Arcs, France, 17–24 March, 2001, http://moriond.in2p3.fr/QCD/2001/indexp.html.
[12] Y. Yamada, K. Hagiwara, and S. Matsumoto, Prog. Theor. Phys. Suppl. **123**, 195 (1996); J. Erler and D.M. Pierce, Nucl. Phys. B **526**, 53 (1998).
[13] M. Carena, S. Mrenna and C.E.M. Wagner, Phys. Rev. D **60**, 075010 (1999).
[14] C. Balazs, J.L. Diaz-Cruz, H.J. He, T. Tait and C.P. Yuan, Phys. Rev. D **59**, 055016 (1999).
[15] Physics at Run II Workshop: Higgs Boson Working Group Report, http://fnth37.fnal.gov/higgs.html.
[16] A. Belyaev, T. Han and R. Rosenfeld, arXiv:hep-ph/0204210.
[17] H. Baer, C.-H. Chen, M. Drees, F. Paige, and X. Tata, Phys. Rev. D **58**, 075008 (1998); M. Guchait and D.P. Roy, Phys. Lett. B **535**, 243 (2002).
[18] C. Hamzaoui, M. Pospelov, and M. Toharia, Phys. Rev. D **59**, 095005 (1999); K.S. Babu and C. Kolda, Phys. Rev. Lett. **84**, 228 (2000); C.-S. Huang, Wei Liao, Q.-S. Yan, and S.-H. Zhu, Phys. Rev. D **63**, 114021 (2001), Erratum-ibid. D **64**, 059902 (2001).
[19] A. Dedes, H.K. Dreiner, U. Nierste, and P. Richardson, arXiv:hep-ph/0207026.
[20] J.F. Gunion, L. Poggioli, R. Van Kooten, C. Kao and P. Rowson, arXiv:hep-ph/9703330.
[21] CMS Collaboration, Technical Proposal, CERN/LHCC/94–38 (1994).
[22] ATLAS Collaboration, ATLAS Detector and Physics Performance: Technical Design Report, CERN/LHCC/99–14 and 99–15 (1999).
[23] T. Plehn, D. Rainwater, and D. Zeppenfeld, Phys. Lett. B **454**, 297 (1999); Phys. Rev. D **61**, 093005 (2000).
[24] K.A. Assamagan, Y. Coadou and A. Deandrea, Eur. Phys. J. direct C **4**, 9 (2002) [arXiv:hep-ph/0203121].
[25] H. Baer, C.-H. Chen, M. Drees, F. Paige and X. Tata, Phys. Rev. D **59**, 055014 (1999).
[26] D. Denegri, W. Majerotto and L. Rurua, Phys. Rev. D **60**, 035008 (1999); I. Hinchliffe and F.E. Paige, Phys. Rev. D **61**, 095011 (2000).
[27] J.L. Feng, M.E. Peskin, H. Murayama and X. Tata, Phys. Rev. D **52**, 1418 (1995).
[28] V.D. Barger, Tao Han, and J. Kelly, Phys. Lett. B **419**, 233 (1998).
[29] S.Y. Choi, A. Djouadi, H.S. Song and P.M. Zerwas, Eur. Phys. J. C **8**, 669 (1999); V. Barger, T. Han, T. Li and T. Plehn, Phys. Lett. B **475**, 342 (2000).
[30] M.M. Nojiri, Phys. Rev. D **51**, 6281 (1995); M.M. Nojiri, K. Fujii and T. Tsukamoto, Phys. Rev. D **54**, 6756 (1996).
[31] E. Boos, G. Moortgat-Pick, H.U. Martyn, M. Sachwitz and A. Vologdin, arXiv:hep-ph/0211040.
[32] A. Djouadi, J. Kalinowski, P. Ohmann and P.M. Zerwas, Z. Phys. C **74**, 93 (1997).
[33] J.F. Gunion and J. Kelly, Phys. Rev. D **56**, 1730 (1997) [arXiv:hep-ph/9610495].
[34] J. F. Gunion and J. Kelly, arXiv:hep-ph/9610421, published in *Snowmass 1996, New Directions for High-energy Physics*, Snowmass, CO, 25 June – 12 July, 623–636 (1996).
[35] J.L. Feng and T. Moroi, Phys. Rev. D **56**, 5962 (1997) [arXiv:hep-ph/9612333].
[36] V. Barger, T. Han and J. Jiang, Phys. Rev. D **63**, 075002 (2001) [arXiv:hep-ph/0006223].
[37] V. Barger, M.S. Berger, J.F. Gunion and T. Han, Phys. Rev. Lett. **75**, 1462 (1995); V. Barger, M.S. Berger, J.F. Gunion and T. Han, Phys. Rept. **286**, 1 (1997).
[38] J. Gunion, T. Han, J. Jiang, S. Mrenna and A. Sopczak, in *Proc. Summer Study on the Future of Particle Physics* (Snowmass 2001), arXiv:hep-ph/0112334.
[39] Y. Yamada, Phys. Lett. B **530**, 174 (2002).

[40] L3 Coll., contributed paper EPS098, Int. Europhysics Conf. on HEP, Brussels, Belgium, 27 July – 2 Aug. 1995.
[41] ALEPH Coll., contributed paper PA13-027, XXVIII Rochester Int. Conf. on HEP, Warsaw, Poland, July 1996.
[42] DELPHI Coll., contributed paper 7-120, Int. Europhysics Conf. on HEP, Tampere, Finland, July 1999;
DELPHI 2001-068 CONF 496, contributed paper for EPS HEP 2001 (Budapest) and LP01 (Rome).
[43] OPAL Coll., OPAL Physics Note PN 483, contributed paper for EPS HEP 2001 (Budapest) and LP01 (Rome).
[44] M. Berggren, R. Keranen and A. Sopczak, EPJdirect C **8**,1 (2000).
[45] A. Sopczak, L3 computing documentation, EGLB (1995), unpublished.
[46] T. Sjöstrand, http://www.thep.lu.se/tf2/staff/torbjorn/LCphysgen.html
[47] J. Kalinowski and M. Krawczyk, Phys. Lett. B **361**, 66 (1995); Physica Pol. B **27**, 961 (1996).
[48] A. Djouadi, J. Kalinowski and P.M. Zerwas, Z. Phys. C **54**, 255 (1992).
[49] B. Grzadkowski, J.F. Gunion and J. Kalinowski, Phys. Rev. D **60**, 075011 (1999) [arXiv:hep-ph/9902308].
[50] M. Berggren, http://home.cern.ch/b/berggren/www/sgv.html
[51] 'Conceptual Design Report of a 500 GeV e^+e^- Linear Collider with Integrated X-ray Laser Facility', DESY 1997-048.
[52] A. Pukhov *et al.*, CompHEP 41.10 [arXiv:hep-ph/9908288].
[53] M. Carena, S. Mrenna and C.E. Wagner, Phys. Rev. D **60**, 075010 (1999) [arXiv:hep-ph/9808312].
[54] S. Dittmaier, M. Krämer, Y. Liao, M. Spira, P.M. Zerwas, Phys. Lett. B **478**, 247 (2000) [arXiv:hep-ph/0002035].
[55] L. Reina and S. Dawson, Phys. Rev. Lett. **87**, 201804 (2001) [arXiv:hep-ph/0107101].
[56] A. Djouadi, J. Kalinowski and M. Spira, Comput. Phys. Commun. **108**, 56 (1998) [arXiv:hep-ph/9704448].
[57] V. Drollinger and A. Sopczak, EPJ C-N **1**, 1 (2001).
[58] B. Grzadkowski, J.F. Gunion and J. Kalinowski, Phys. Lett. B **480**, 287 (2000) [arXiv:hep-ph/0001093].
[59] A. Sopczak, Z. Phys. C **65**, 449 (1995).
[60] M. Battaglia, A. Ferrari, A. Kiiskinen, T. Maki, LC-note E305, arXiv:hep-ex/0112015.
[61] J. Guasch, W. Hollik and A. Kraft, Nucl. Phys. B **596**, 66 (2001).
[62] F. Gianotti *et al.*, arXiv:hep-ph/0204087.
[63] S. Dawson, D. Dicus and C. Kao, Phys. Lett. B **545**, 132 (2002) [arXiv:hep-ph/0208063].
[64] P. Chankowski, T. Farris, B. Grzadkowski, J.F. Gunion, J. Kalinowski and M. Krawczyk, Phys. Lett. B **496**, 195 (2000). [arXiv:hep-ph/0009271].
[65] However, we emphasize that the above LHC versus LC comparisons have been made based only on $H, A, H^{\pm}$ processes and for the particular choice of $m_A = 200$ GeV in the MSSM, assuming $\sqrt{s} = 500$ GeV for the LC. It is very possible that the relative accuracies as a function of $\tan\beta$ could be quite different if the LC energy is such that $m_A > \sqrt{s}/2$, since then HA and H^+H^- pair production would not be possible.